Glucose Analogue Inhibitors of Glycogen Phosphorylase: The Design of Potential Drugs for Diabetes[†,‡]

J. L. Martin,[§] K. Veluraja,[§] K. Ross,[§] L. N. Johnson,*[,§] G. W. J. Fleet,[∥] N. G. Ramsden,[∥] I. Bruce,[∥] M. G. Orchard,[∥] N. G. Oikonomakos,[⊥] A. C. Papageorgiou,[⊥] D. D. Leonidas,[⊥] and H. S. Tsitoura[⊥]

Laboratory of Molecular Biophysics, The Rex Richards Building, South Parks Road, Oxford OX1 3QU, U.K., Dyson Perrins Laboratory, South Parks Road, Oxford OX1 3QU, U.K., and The National Hellenic Foundation, 48, Vas. Constantinou Avenue, Athens 11635, Greece

Received June 7, 1991; Revised Manuscript Received August 7, 1991

ABSTRACT: The T-state crystal structure of the glucose–phosphorylase *b* complex has been used as a model for the design of glucose analogue inhibitors that may be effective in the regulation of blood glucose levels. Modeling studies indicated room for additional atoms attached at the C1-β position of glucose and some scope for additional atoms at the C1-α position. Kinetic parameters were determined for α-D-glucose: K_i = 1.7 mM, Hill coefficient n = 1.5, and α (synergism with caffeine) = 0.2. For β-D-glucose, K_i = 7.4 mM, n = 1.5, and α = 0.4. More than 20 glucose analogues have been synthesized and tested in kinetic experiments. Most were less effective inhibitors than glucose itself and the best inhibitor was α-hydroxymethyl-1-deoxy-D-glucose (K_i = 1.5 mM, n = 1.3, α = 0.4). The binding of 14 glucose analogues to glycogen phosphorylase *b* in the crystal has been studied at 2.4-Å resolution and the structure have been refined to crystallographic *R* values of less than 0.20. The kinetic and crystallographic studies have been combined to provide rationalizations for the apparent affinities of glucose and the analogues. The results show the discrimination against β-D-glucose in favor of α-D-glucose is achieved by an additional hydrogen bond made in the α-glucose complex through water to a protein group and an unfavorable environment for a polar group in the β pocket. The compound α-hydroxymethyl-1-deoxy-D-glucose has an affinity similar to that of glucose and makes a direct hydrogen bond to a protein group. Comparison of analogues with substituent atoms that have flexible geometry (e.g., 1-hydroxyethyl β-D-glucoside) with those whose substituent atoms are more rigid (e.g., β-azidomethyl-1-deoxyglucose or β-cyanomethyl-1-deoxyglucose) indicates that although all three compounds make similar polar interactions with the enzyme, those with more rigid substituent groups are better inhibitors. In another example, α-azidomethyl-1-deoxyglucose was a poor inhibitor. In the crystal structure the compound made several favorable interactions with the enzyme but bound in an unfavorable conformation, thus providing an explanation for its poor inhibition. Attempts to utilize a contact to a buried aspartate group were partially successful for a number of compounds (β-aminoethyl, β-mesylate, and β-azidomethyl analogues). The β pocket was shown to bind gentiobiose (6-*O*-β-D-glucopyranosyl-D-glucose), indicating scope for binding of larger side groups for future studies.

Diabetes mellitus is characterized by chronic elevated blood glucose levels. The disorder affects 1–2% of the population in the Western world, and 75% of this total is accounted for by the non-insulin-dependent form of the disease (NIDDM or Type II diabetes). NIDDM is managed by diet, exercise, hypoglycemic drugs, and, if these fail, insulin therapy. Treatment is not entirely satisfactory since it is difficult to control blood glucose concentrations as effectively as in normal subjects. Failure to provide good control of the blood glucose level over several years can result in the complications that occur in the later life of diabetic patients and there is a continued interest in new agents which more closely mimic the physiological control of blood glucose levels.

Hyperglycemia in NIDDM patients is a result of diminished insulin release and/or insulin resistance that leads to impaired tissue glucose uptake and impaired suppression of hepatic glucose production (DeFronzo, 1988). In response to insulin release after a meal, muscle glycogen synthesis is the principal pathway of glucose disposal and defects in muscle glycogen synthesis have a dominant role in the insulin resistance that occurs in persons with NIDDM (Lillioja et al., 1986; Shulman et al., 1990). At basal insulin levels, impaired suppression of hepatic output of glucose arising from gluconeogenesis and glycogen breakdown is the principal cause of the high glucose concentrations in NIDDM patients. In the animal model (the genetically diabetic *db/db* mouse), the activity of hepatic phosphorylase is increased compared with nondiabetic mice (Roesler & Khandelwal, 1985; Bollen et al., 1983). Weak inhibitors of glycogen phosphorylase are weakly hypoglycemic (Kasvinsky et al., 1978b). Amylin, the major component of amyloid fibers in the pancreas of NIDDM patients, causes a dose-dependent increase in phosphorylase activity (Young et al., 1991). These observations suggest that inhibitors of glycogen phosphorylase may help shift the balance between glycogen synthesis and glycogen degradation in favor of glycogen synthesis in both muscle and liver and may be useful therapeutic agents for treatment of diabetes.

Glycogen phosphorylase catalyzes the first step in the phosphorolysis of glycogen to yield glucose 1-phosphate

[†] This work has been supported by the Oxford Centre for Molecular Sciences.

[‡] Coordinates for the glucose–phosphorylase *b* complex have been deposited with the Brookhaven Protein Data Bank, Chemistry Department, Brookhaven National Laboratory, Upton, NY 11973, from which copies are available.

* Author to whom correspondence should be addressed.
[§] Laboratory of Molecular Biophysics.
[∥] Dyson Perrins Laboratory.
[⊥] The National Hellenic Foundation.

0006-2960/91/0430-10101$02.50/0

Chart I

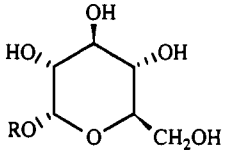

(1) R = H
(4) R = Me
(6) R = CH_2CH_2OH

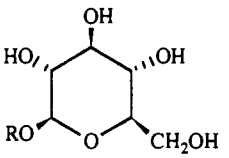

(2) R = H
(5) R = Me
(7) R = CH_2CH_2OH

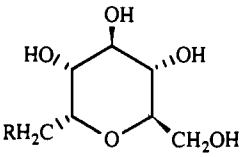

(3) R = H
(8) R = N_3
(12) R = OH
(16) R = OSO_2Me
(19) R = NH_3+

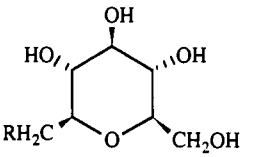

(9) R = N_3
(11) R = CH_2N_3
(13) R = OH
(15) R = CH_2OH
(17) R = OSO_2Me
(20) R = NH_3+
(21) R = CH_2NH_3+
(22) R = CN

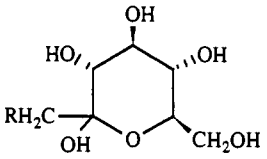

(10) R = N_3
(14) R = OH
(18) R = OSO_2Me
(23) R = CN

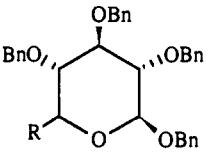

(25) R = OH
(26) R = Cl
(27) R = α-OCH_2CH_2OH
(28) R = β-OCH_2CH_2OH

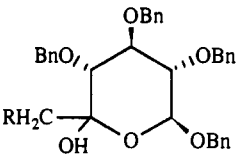

(29) R = OH
(30) R = OSO_2Me
(31) R = CN

Bn = $PhCH_2$

(Glc-1-P),[1] which is utilized via glycolysis to provide energy to sustain muscle contraction and in the liver is converted to glucose to supply energy for extrahepatic tissues. Phosphorylase is an archetypal control enzyme and exists in two (or at least two) interconvertible states, a T state that exhibits low activity and low affinity for substrate and an R state that exhibits high activity and high affinity for substrate. In the liver the major control mechanism is through reversible phosphorylation that converts the inactive *b* form of the enzyme (T state) to the active *a* form (R state). In muscle, control of phosphorylase is exerted both by reversible phosphorylation in response to nervous or hormonal signals and through noncovalent binding of allosteric effectors. Glucose is a physiological regulator of hepatic glycogen metabolism that promotes inactivation of glycogen phosphorylase (Stalmans et al., 1974; Hers, 1976) and acts synergistically with insulin (Witters & Avruch, 1978; Hartman et al., 1987). Glucose inactivates phosphorylase *a* (GP*a*) by competitive inhibition with Glc-1-P and by stabilization of the T-state conformation of the enzyme, which is a better substrate than the R-state conformation for the dephosphorylation reaction catalyzed by phosphatase I (Bailey & Whelan, 1972; Madsen et al., 1978, 1983; Sprang et al., 1982b). Diminished concentrations of GP*a* allow the phosphatase to activate glycogen synthase. Muscle GP*a* exhibits similar regulation by glucose in vitro but this regulation may not be significant in vivo since rapid phosphorylation on uptake ensures that there are negligible concentrations of free glucose in muscle. Recent evidence has shown that in muscle insulin stimulates glycogen synthase activity through stimulation of phosphatase 1 (Dent et al., 1990). Insulin also stimulates dephosphorylation of GP*a* (Zhang et al., 1989) although possibly by a different activation mechanism of phosphatase 1 to that observed for dephosphorylation of glycogen synthase (Dent et al., 1990).

We report the design and experimental investigation of a number of glucose analogue inhibitors of glycogen phosphorylase based on the known three-dimensional structure of T-state rabbit muscle GP*b* (Acharya et al., 1991). The constellations of atoms at the catalytic sites of T-state GP*a* and T-state GP*b* are very similar (Sprang et al., 1988b), and both GP*a* and GP*b* exhibit similar inhibition constants for glucose (K_i approximately 2 mM) (Sprang et al., 1982; Street et al., 1986). The three-dimensional structure of liver phosphorylase is not known, but the amino acid sequence (Newgard et al., 1986) is 80% identical to the sequence of the muscle enzyme overall and 100% identical for all residues involved in the catalytic site.

Experimental Procedures

Modeling. Possible interaction sites at the catalytic site of GP*b* were identified with GRID (Goodford, 1984, 1985; Boobyer et al., 1989), a program that calculates the nonbonded interaction energy between a chemical functional group (the probe) and the macromolecule at a number of regularly spaced positions. The interaction energy comprises terms for Lennard-Jones, electrostatic, and hydrogen-bond energies. The coordinates for GP*b* were those resulting from the refinement of the native T-state structure at 1.9-Å resolution (Acharya et al., 1991). A number of different probes (methyl, hydroxyl, and amine groups) were used with a grid interval of 0.33 Å within the vicinity of the catalytic site. Contours of +1 kcal/mol (slightly repulsive energy) were used to display the shape and extent of the catalytic site cavity and contours of between −5 and −15 kcal/mol (depending on the probe group) to display potential favorable binding sites. Modeling of compound **6** (see next section for definition) was performed by maintaining the glucose structural framework in its bound conformation at the catalytic site (Martin et al., 1990) and adding substituents to interact with the protein at the favorable GRID-predicted binding sites. Modeling of other compounds was performed by keeping constant the glucosyl part of the structure in its bound conformation and varying the torsion angles for the substituent groups. Those compounds that gave

[1] Abbreviations: BES, *N,N*-bis[2-hydroxyethyl]-2-aminoethanesulfonic acid; DTT, dithiothreitol; Glc-1-P, α-D-glucose 1-phosphate; gentiobiose, 6-*O*-β-D-glucopyranosyl-D-glucose; PLP, pyridoxal 5′-phosphate; GP*a* and GP*b*, glycogen phosphorylase (E.C. 2.4.1.1) *a* and *b*, respectively; GBP, *Escherichia coli* periplasmic D-galactose(glucose) binding protein.

favorable van der Waals interactions and had satisfactory steric energy were considered for synthesis and testing.

Materials. AMP, glucose 1-phosphate (as the dipotassium salt), α-(**1**) and β-(**2**) D-glucose, the methyl glucosides (**4** and **5**), gentiobiose (**24**), and 2,3,4,6-tetra-*O*-benzyl-glucopyranose (**25**) were purchased from Sigma (Chart I). The glucose analogues **3**, **8**, **9**, **11**, **12**, **13**, **15**, **16**, **17**, **19**, **20**, **21**, and **22** were prepared as described elsewhere (Bruce et al., manuscript in preparation).

The 2-hydroxyethyl glucopyranosides (**6** and **7**) were prepared by conversion of the protected glucopyranose (**25**) to the glucopyranosyl chloride (**26**) by a modification of the published procedure (Austin et al., 1964). Thus, 2,3,4,6-tetra-*O*-benzylglucopyranose (**25**) (374 mg, 0.69 mmol) was dissolved in thionyl chloride (2 mL), and the reaction was stirred at 50 °C until evolution of gases had ceased. Solvents were removed under reduced pressure, and toluene (2 × 5 mL) was distilled from the residue. Pyridine (279 μL, 3.45 mmol) and ethane-1,2-diol (192 μL, 3.45 mmol) were added to a solution of the crude pyranosyl chloride (**26**) in dichloromethane (5 mL). The reaction mixture was cooled to 0 °C and stirred in the dark with silver trifluoromethanesulfonate (886 mg, 3.45 mmol). The reaction was allowed to warm to room temperature over 4 h and then stirred in the light to precipitate silver salts for 1 h. The reaction was washed with 2 M aqueous hydrochloric acid (25 mL) and water (25 mL). Solvents were removed under reduced pressure and the residue was purified by repeated flash column chromatography (ether/hexane 1:1) to give the protected 2-hydroxyethyl α-(**27**) (137 mg, 34% yield), and β-(**28**) (117 mg, 29%) glucopyranosides.

2-Hydroxyethyl β-D-Glucopyranoside (**7**). The protected β-D-glucopyranoside (**28**) (117 mg, 0.2 mmol) was dissolved in freshly distilled methanol (5 mL) and a catalytic amount of palladium black was added. The reaction was stirred under hydrogen for 24 h. The reaction was filtered through Celite and the solvents were removed under reduced pressure. The residue was recrystallized from ethanol/acetone to yield 2-hydroxyethyl β-D-glucopyranoside (**7**), (41 mg, 91%), mp 136–138 °C [lit. mp 136–138 °C (Karjala, 1940)]; ^{13}C NMR (C_5D_5N) δ_C 98.0 (d), 71.5 (d), 68.3 (d), 65.3 (t), 64.6 (d), 55.6 (t), 54.9 (t); ^{1}H NMR (C_5D_5N) δ_H 4.54 (d, 1 H, H-1, J = 7.2 Hz), 4.16 (dd, 1 H), 4.01–3.78 (m, 4 H), 3.74–3.49 (m, 5 H); m/z (DCI NH_3) 242 ($M + NH_4^+$, 70%), 180 [$M - (CH_2OH)_2 + NH_4^+$].

2-Hydroxyethyl α-D-Glucopyranoside (**6**). The protected α-D-glucopyranoside (**27**) (137 mg, 0.23 mmol) was dissolved in freshly distilled methanol (5 mL) and a catalytic amount of palladium black was added. The reaction was stirred under hydrogen for 24 h. The reaction was filtered through Celite and the solvents were removed under reduced pressure. The residue was recrystallized from ethanol/ethyl acetate to afford 2-hydroxyethyl α-D-glucopyranoside (**6**) (48 mg, 91%), mp 100–104 °C [lit. mp 100–102 °C (Helfrich et al., 1960)]; ^{13}C NMR (C_5D_5N) δ_C 94.7 (d), 69.4 (d), 68.3 (d), 67.8 (d), 66.1 (t), 64.7 (d), 56.7 (t), 55.4 (t); ^{1}H NMR (C_5D_5N) δ_H 5.35 (d, 1 H, H-1, J = 3.6 Hz), 4.7–3.7 (m, 10 H); m/z (DCI NH_3) 242 ($M + NH_4^+$ + 80%), 180 [$M - (CH_2OH)_2 + NH_4^+$].

Glucoheptulose (**14**). 3,4,5,7-Tetra-*O*-benzyl-α-D-*gluco*-heptulopyranose (**29**) (Aebischer et al., 1982; Noort et al., 1990) (146 mg, 0.256 mmol) in methanol (4 mL) was stirred, under hydrogen, in the presence of palladium black (13 mg) for 8 h at room temperature, whereupon tlc (ethyl acetate/methanol 5:1) indicated the presence of a single product (R_f 0.1). The suspension was then filtered through Celite and the solvent was removed under vacuum. The crude product was purified by flash chromatography (ethyl acetate/methanol 5:1 grading to 1:1) to give α-D-*gluco*-heptulopyranose (**14**) (33 mg, 61%), as a colorless gum; ^{13}C NMR (D_2O) δ_C 61.4, 64.4 (2t, $2CH_2O$), 70.2, 71.0, 73.0, 74.4 (4d, 4CHO), 98.2 (s, C-2). [lit. ^{13}C NMR (D_2O) δ_C 61.6 (t, C-7), 64.6 (t, C-1), 70.4 (d, C-5), 71.2 (d, C-3), 73.1 (d, C-6), 74.3 (d, C-4), 98.1 (s, C-2) (Angyal et al., 1983)].

1-O-Methanesulfonyl-3,4,5,7-tetra-O-benzyl-α-D-gluco-heptulopyranose (**30**). Mesyl chloride (0.25 mL, 3.23 mmol) was added to a stirred solution of 3,4,5,7-tetra-*O*-benzyl-α-D-*gluco*-heptulopyranose (**29**) (560 mg, 0.98 mmol) in dry pyridine (3 mL) at 0 °C under nitrogen. The mixture was then allowed to reach room temperature, whereupon tlc (hexane/ethyl acetate 1:1) indicated complete consumption of the starting material (R_f 0.3) and a single product (R_f 0.5). The reaction mixture was diluted with ether and washed successively with 2 M aqueous hydrochloric acid (30 mL), water, and then brine. The solvent was removed under vacuum and the crude product was purified by flash chromatography (hexane/ethyl acetate 2:1) to give 1-*O*-methanesulfonyl-3,4,5,7-tetra-*O*-benzyl-α-D-benzyl-α-*gluco*-heptulopyranose (**30**) (617 mg, 97%) as a colorless gum; $[\alpha]_D^{20}$ +19.2 (*c* 1.0 in $CHCl_3$); IR (film from ether) ν_{max} 3457 (OH) and 1359 (SO_2) cm^{-1}; ^{1}H NMR ($CDCl_3$) δ_H 2.95 (3 H, s, SO_2CH_3), 3.20 (1 H, s, OH), 3.72 (4 H, m), 3.99 (2 H, m), 4.07 (1 H, d, H-1, $J_{1-1'}$ = 11.5 Hz), 4.22 (1 H, d, H-1′, $J_{1-1'}$ = 11.5 Hz), 4.50 (2 H, m), 4.66 (2 H, m), 4.91 (4 H, m), 7.32 (20 H, m, Ph); ^{13}C NMR ($CDCl_3$) δ_C 37.9 (q, SO_2CH_3), 68.5, 70.6, 73.4, 75.0, 76.5, 75.7 (6t, $6CH_2O$), 71.6, 77.9, 78.4, 83.1 (4d, 4CHO), 96.1 (s, C-2); m/z (DCI, NH_3) 666 ($M + NH_4^+$, 10%), 570 ($M - CH_3SO_3H + NH_4^+$, 10%), 91 ($PhCH_2^+$, 100%). Anal. Calcd for $C_{36}H_{40}O_9Si$: C, 66.65; H, 6.21. Found: C, 66.73; H, 6.40.

1-O-Methanesulfonyl-α-D-gluco-heptulopyranose (**18**). The protected mesylate (**30**) (382 mg, 0.589 mmol) in methanol (6 mL) was stirred, under hydrogen, in the presence of palladium black (60 mg) for 30 h at room temperature, whereupon tlc (ethyl acetate/methanol 5:1) indicated the presence of a single product (R_f 0.3). The suspension was then filtered through Celite and the solvent was removed under vacuum. The crude product was purified by flash chromatography (ethyl acetate/methanol 5:1) to give 1-*O*-methanesulfonyl-α-D-*gluco*-heptulopyranose (**18**) (163 mg, 95%) as a colorless gum; $[\alpha]_D^{20}$ +37.8 (*c* 1.0 in H_2O); IR (film from THF) ν_{max} 3369 (OH) and 1348 (SO_2) cm^{-1}; ^{1}H NMR (D_2O) δ_H 3.05 (3 H, s, SO_2CH_3), 3.21 (1 H, t, J = 9.4 Hz), 3.28 (1 H, d, J = 9.6 Hz), 3.58 (4 H, m), 4.05 (1 H, d, H-1, $J_{1-1'}$ = 10.6 Hz), 4.17 (1 H, d, H-1′, $J_{1-1'}$ = 10.6 Hz); ^{13}C NMR (D_2O) δ_C 37.4 (q, SO_2CH_3), 61.2 (t, C-7), 71.1 (t, C-1), 70.1, 71.3, 73.5, 74.1 (4t, 4CHO), 96.6 (s, C-2); m/z (DCI, NH_3) 306 ($M + NH_4^+$, 2%), 288 ($M - H_2O + NH_4^+$, 100%). Anal. Calcd for $C_8H_{16}O_9S$: C, 33.33; H, 5.59. Found: C, 33.37; H, 5.68.

1-Azido-1-deoxy-α-D-gluco-heptulopyranose (**10**). A mixture of sodium azide (15 mg, 0.23 mmol) and the mesylate (**18**) (45 mg, 0.156 mmol) in dry dimethylformamide (1 mL) was stirred at room temperature under nitrogen for 4 days, whereupon tlc (chloroform/methanol 4:1) indicated complete consumption of the starting material (R_f 0.13) and a single product (R_f 0.18). The solvent was removed under vacuum, and a solution of the residue in chloroform was adsorbed onto silica gel. The product was then eluted through a short silica gel column using chloroform/methanol (4:1) to give 1-azido-1-deoxy-α-D-*gluco*-heptulopyranose (**10**) (35 mg, 95%) as

a colorless foam; $[\alpha]_D^{20}$ +43.5 (*c* 1.0 in H_2O); IR (film) ν_{max} 3369 (OH) and 2111 (N_3) cm^{-1}; ^1H NMR (D_2O) δ_H 3.25 (1 H, t, J = 9.5 Hz), 3.31 (2 H, m, H-1 and H-1′), 3.32 (1 H, d, J = 9.0 Hz), 3.62 (4 H, m); ^{13}C NMR (D_2O) δ_C 55.3 (t, C-1), 61.3 (t, C-7), 70.2, 72.0, 73.3, 74.2 (4t, 4CHO), 98.3 (s, C-2); *m/z* (DCI, NH_3) 253 (M + NH_4^+, 100%). Anal. Calcd for $C_7H_{13}N_3O_6$: C, 35.75; H, 5.57; N, 17.87. Found: C, 35.52; H, 5.73; N, 17.60.

3,4,5,7-Tetra-O-benzyl-1-cyano-1-deoxy-α-D-gluco-heptulopyranose (**31**). A mixture of sodium cyanide (39 mg, 0.80 mmol) and the protected mesylate (**30**) (236 mg, 0.364 mmol) in dry dimethylformamide (2 mL) was stirred at room temperature under nitrogen for 1 h, whereupon tlc (hexane/ethyl acetate 2:1) indicated complete consumption of the starting material (R_f 0.2) and a single product (R_f 0.3). The mixture was diluted with ether, washed several times with water, and dried over sodium sulfate, and the solvent was evaporated under a vacuum to give a pale yellow gum. The crude product was dissolved and eluted through a short silica gel column using hexane/ethyl acetate (2:1) as solvent to give 3,4,5,7-tetra-*O*-benzyl-1-cyano-1-deoxy-α-D-*gluco*-heptulopyranose (**31**) (205 mg, 97%), as a colorless gum; $[\alpha]_D^{20}$ +2.0 (*c* 1.0 in $CHCl_3$); IR (film from ether) ν_{max} 3401 (OH) and 2255 (CN) cm^{-1}; ^1H NMR ($CDCl_3$) δ_H 2.50 (1 H, d, H-1, $J_{1-1'}$ = 16.5 Hz), 2.66 (1 H, d, H-1′, $J_{1-1'}$ = 16.5 Hz), 3.24 (1 H, s, OH), 3.58 (1 H, d, J = 9.1 Hz), 3.75 (3 H, m), 3.97 (2 H, m), 4.78 (8 H, m), 7.35 (20 H, m, Ph); ^{13}C NMR ($CDCl_3$) δ_C 28.4 (t, CH_2CN), 68.3, 73.4, 75.1, 75.5, 75.6 (5t, $5CH_2O$), 72.5, 78.0, 80.0, 83.3 (4d, 4CHO), 96.0 s, OCOH), 116.1 (s, CN); *m/z* (DCI, NH_3) 597 (M + NH_4^+, 11%), 91 ($PhCH_2^+$, 100%). Anal. Calcd for $C_{36}H_{37}NO_6$: C, 74.59; H, 6.43; N, 2.42. Found: C, 74.45; H, 6.33; N, 2.54.

1-Cyano-1-deoxy-α-D-gluco-heptulopyranose (**23**). The protected nitrile (**31**) (153 mg, 0.264 mmol) in methanol (4 mL) was stirred, under hydrogen, in the presence of palladium black (46 mg) and camphorsulfonic acid (4 mg) for 10 h at room temperature, whereupon tlc (ethyl acetate/methanol 5:1) indicated the presence of a single product (R_f 0.3). The suspension was then filtered through Celite and the solvent was removed under vacuum. The crude product was purified by flash chromatography (ethyl acetate/methanol 5:1) to give 1-cyano-1-deoxy-α-D-*gluco*-heptulopyranose (**23**) (50 mg, 86%) as a white solid (after freeze-drying); $[\alpha]_D^{20}$ +70.3 (*c* 1.0 in H_2O); IR (film from THF) ν_{max} 3369 (OH) and 2261 (CN) cm^{-1}; (D_2O) δ_H 3.21 (3 H, m), 3.55 (5 H, m); (D_2O) δ_C 28.2 (t, CH_2CN), 61.1 (t, C-8), 70.1, 73.7, 74.0, 74.2 (4d, 4CHO), 96.6 (s, OCOH) 118.4 (s, CN); *m/z* (DCI, NH_3) 237 (M + NH_4^+, 67%).

Kinetic Studies. GP*b* was isolated from rabbit skeletal muscle according to the method of Fischer and Krebs (1962) but using 2-mercaptoethanol instead of L-cysteine. The enzyme was recrystallized at least four times and bound nucleotides were removed as described by Melpidou and Oikonomakos (1983). Protein concentration was determined from absorbance mesurements at 280 nm using the specific absorbance coefficient [ϵ = 13.2 for a 1% solution in a cell of path length 1 cm (Kastenschmidt et al., 1968)].

The glucose analogues were freshly dissolved immediately before use. Oyster glycogen (Serva) was freed of AMP using the method of Helmreich and Cori (1964). Phosphorylase activity in the direction of glycogen synthesis was determined at pH 6.8 and 30 °C by measuring the inorganic phosphate released in the reaction (Fiske & Subbarow, 1925). The enzyme (5–20 μg/mL) was assayed in 47 mM triethanolamine hydrochloride (pH 6.8), 100 mM KCl, 1 mM DTT, 1 mM EDTA, 1% glycogen, and 1 mM AMP with concentrations of Glc-1-P between 3 and 20 mM and concentrations of glucose analogues as indicated in the results. Enzyme and glycogen were preincubated for 15 min at 30 °C before the reaction was initiated with the "substrate" mixtures containing AMP and Glc-1-P with or without inhibitor. Final assay volumes were between 0.25 and 0.5 mL. Initial velocities were calculated from the pseudo-first-order reaction constants (Engers et al., 1970). The kinetic experiments with α- and β-D-glucose were completed within 2 min of dissolution to minimize anomerization. Assay times were 1 min and the enzyme concentration was raised to 25 μg/mL.

Enzyme preparations exhibited V_{max} values of 70–80 μmol mg^{-1} min^{-1} (with respect to Glc-1-P) and K_m values for Glc-1-P of 1.5–2.2 mM at saturating AMP (1 mM) and glycogen (1%). Kinetic data were analyzed by Michaelis–Menten kinetics using a nonlinear regression data analysis (Leatherbarrow, 1987, 1990) assuming that each rate is subject to about the same proportion of random error (Cornish-Bowden & Wharton, 1988). The program calculates K_m and V_{max} and the standard errors for these values. Hill (or Dixon) plots were generated by linear regression analysis (Leatherbarrow, 1987) using the same type of error distribution, but in this case, the program only calculates the standard errors of the slopes and intercepts. Standard errors for K_m(app) were therefore calculated using known relations between standard errors. K_i values were determined by plotting K_m(app) (slopes or intercepts) versus inhibitor concentration (Segel, 1975) with an explicit value for the standard deviation of each point.

The parent compounds and glucose analogues were also tested for synergistic inhibition with caffeine either by using various concentrations of the analogue and various concentrations of caffeine at constant concentrations of Glc-1-P (10 mM), glycogen (1%), and AMP (1 mM) or by using a single concentration of the analogue (10 mM), a single constant concentration of caffeine (0.15 mM), and various concentrations of Glc-1-P. In the first case the interaction constant, α (Segal, 1975), was calculated from Dixon plots as described previously (Kasvinsky et al., 1978; Papageorgiou et al., 1989, 1991). In the second case the interaction constant was calculated from the equation $K_m(app) = K_m(1 + [I]/K_i + [X]/K_x + [I][X]/\alpha K_i K_x)$ where I is caffeine, X is analogue, K_i and K_x are their corresponding inhibition constants (determined separately), and K_m(app) is the apparent K_m for the substrate determined in the presence of both I and X. According to Segal (1975), in a synergistic competitive inhibition by two different nonexclusive inhibitors, the binding of one inhibitor may ($\alpha < 1$) or may not ($\alpha = 1$) affect the binding of the other.

Crystallographic Binding Studies. T-state GP*b* was crystallized from the purified protein in a medium consisting of 20–40 mg/mL GP*b*, 1 mM IMP, 1 mM spermine, 10 mM BES, 0.1 mM EDTA, and 0.02% sodium azide (pH 6.7) (Oikonomakos et al., 1985) to give tetragonal crystals, space group $P4_32_12$, unit cell dimensions $a = b$ = 128.5 Å and c = 116.3 Å. Prior to data collection, crystals were soaked in a buffered solution (10 mM BES, 0.1 mM EDTA, and 0.02% sodium azide, pH 6.7) containing the glucose analogue inhibitor at a concentration of 100 mM for times between 0.5 and 2 h. Data of 2.3 Å were collected on a Nicolet IPC multiwire area detector (Howard et al., 1987) using a Rigaku RU-200 rotating anode X-ray source, with graphite monochromator, operating at 50 kV and 50 mA or at 60 kV and 60 mA (depending on crystal size). The detector was placed 16 cm away from the crystal and at a swing angle of 22°.

Data frames of 0.2° oscillation were collected with exposure times between 90 and 120 s for a total angular rotation range of at least 90°. Collection times were less than 24 h for almost all experiments. Each experiment was performed using a single crystal of GP*b* (average crystal size 1.6 × 0.5 × 0.5 mm). The data frames were processed with the XENGEN package of programs (A. J. Howard, published results) to produce a scaled set of structure factors, and these were then used to generate difference Fourier electron density maps (with respect to the native protein) using the CCP4 package of crystallographic programs (Daresbury Laboratory, U.K.).

Refinement of the enzyme complexes was performed on a Convex C210 using X-PLOR energy and crystallographic least-squares minimization (tolerance set to 0.05 Å) (Brunger, 1988, 1989; Brunger et al., 1989). Individual atomic *B*-factor refinement was performed in the final cycles with target standard deviations of 1.5 and 2 Å^2 for bonded atoms and for atoms linked by one other atom, respectively. The starting structures of the ligands were taken from structures which had been generated with ideal geometry with torsion angles adjusted to fit the difference Fourier electron density maps. The starting protein structure was the refined structure of the glucose complex comprising residues 14–842 (Martin et al., 1990). Waters from the GP*b*-glucose complex (except those that had been displaced by the ligand) were also included in the refinement. X-PLOR parameters for the ligands and for the pyridoxal phosphate are available from the authors. No simulated annealing refinement was carried out as the difference maps indicated no substantial changes from the GP*b* glucose complex. $2F_o - F_c$ electron density maps, in which the terms were weighted by $\exp[-(|F_o - F_c|/F_o)]$ (Rayment, 1983), were generated from X-PLOR-refined coordinates. F_o and F_c are the observed and calculated structure factor amplitudes, respectively. The maps were examined for satisfactory fit of atoms to density.

Graphics and Structural Analysis. Modeling of ligands and display of maps and structures used the molecular graphics program FRODO (Jones, 1978, 1985; modified by J. W. Pflugrath, M. Saper, R. Hubbard, and P. Evans) implemented on an Evans and Sutherland PS300 or PS390 graphics terminal on-line to a VAX 6210. Hydrogen bonds were assigned by FRODO if the distance between two electronegative atoms was less than 3.3 Å and if the angle between these two atoms and each of the preceding atoms was greater than 90°. Van der Waals interactions were assumed where non-hydrogen atoms are separated by less than 4 Å.

RESULTS

Structural studies with T-state GP*a* and T-state GP*b* (Sprang et al., 1982b; Martin et al., 1990) have shown that glucose binds at the catalytic site, located at the center of the molecule about 15 Å from the surface and close to the essential pyridoxal phosphate cofactor. The sugar makes hydrogen bonds to suitable protein groups through each of the peripheral hydroxyl groups including a hydrogen bond from the α-1-OH via a water molecule to an aspartic acid, Asp283, and a hydrogen bond from 2-OH to Asn284. Conversion of T-state GP*b* to R-state GP*b* or R-state GP*a* results in several changes at the catalytic site, which include a displacement of the 280s loop (residues 282–286) that allows access to the catalytic site and a replacement as Asp283 by Arg569 that leads to the creation of a phosphate recognition site at the catalytic site (Barford & Johnson, 1989; Barford et al., 1991). In the present design of inhibitors we have imposed the constraint that the inhibitor must stabilize the T state of the enzyme and mimic the contacts of glucose that localize the 280s loop. Often the most powerful inhibitors of enzyme-catalyzed reactions are compounds that mimic the transition state. But most transition-state inhibitors of GP (for example, heptulose-2-P) tend to favor the R-state conformation (Johnson et al., 1990). Caffeine is also an inhibitor of GP*b* and GP*a* (K_i = 0.1 mM; Kasvinsky et al., 1978b) and exerts its effects noncompetitively by binding at a site (the nucleoside inhibitor site) some 12 Å from the catalytic site, where it intercalates between two aromatic groups, Phe285 and Tyr613, and stabilizes the T state of the enzyme by localization of the 280s loop (Kasvinsky et al., 1978a). Caffeine and glucose inhibition are synergistic (Kasvinsky et al., 1978b). The nucleotide inhibitor site is known to bind a number of purine analogues or related heterocyclic rings that are also inhibitors of phosphorylase (Sprang et al., 1982a). Although this site offers a further target for inhibitor design and may play a role in insulin regulation (Kasvinsky et al., 1981), it was not explored in the present study.

Modeling Studies. Two different views of the van der Waals surface of α-D-glucose bound to T-state GP*b* are shown in Figure 1, top and middle panels. As seen in the face-on view, Figure 1 (top), all equatorial hydroxyl groups are involved in hydrogen bonds to the enzyme and there is little room for any substitution of additional atoms. There is, however, an empty pocket at the β configuration adjacent to C1 which represents the pocket recognized in the binding studies with D-gluconohydroximo-1,5-lactone *N*-phenylurethane (Barford et al., 1988). The space at the α position (Figure 1, middle) is partially filled with water molecules and leads toward the 280s loop. The GRID interaction energies for an OH probe with the GP*b*–glucose coordinates for protein atoms (but without glucose or water molecules) are shown in Figure 1 (bottom). They predict a favorable hydrogen-bonding site in the vicinity of Asp283 and Gly135. Hydroxyethyl α-D-glucoside (compound **6**, Chart I) was modeled using the known glucose coordinates (Figure 1, bottom). This structure was the starting point for the design, synthesis, and analysis of a series of compounds.

Kinetic Studies. A summary of the kinetic results for the glucose analogue inhibitors is given in Table I. The compounds studied differ only in their substituent atoms at either the α or the β configuration at the C1 position of the glucopyranose ring (Chart I). Experimental points were averages of triplicates deduced from assays of a total volume of 0.5 mL. In several experiments limited quantities of inhibitor were available, so experimental points were averages of duplicates (assay volume 0.25 mL) and only one inhibitor concentration was used. There was some variation in different enzyme preparations represented by a variation in K_m for glucose-1-P (on which determinations of K_i are based) of 1.5–2.2 mM, which is not unusual. Within 1 week the means of the standard errors for the calculated K_ms averaged less than 8%.

Previous work had suggested that glycogen phosphorylase binds α-D-glucose in preference to β-D-glucose (Cori & Cori, 1940). Later studies indicated that both α and β anomers were inhibitors (Ariki & Fukui, 1977). Street et al. (1986), using a single Glc-1-P concentration (4 mM) and an assay completed within 6 min of dissolution, showed that phosphorylase has a 3-fold lower K_i for α-D-glucose than for β-D-glucose (K_i values of 1 mM and 3 mM, respectively). These values, obtained at low substrate concentration, are probably minimum values. In the present study, α and β anomers were tested 2 min after dissolution (1-min assay) at five different substrate concentrations (Table I). Figure 2 shows the effects of 10 mM α-D-glucose or 10 mM β-D-glucose on the activity of GP*b* in the direction of glycogen synthesis. Analysis of the data gave K_i values of 1.7 mM and 7.4 mM for α-D-glucose and β-D-

Table I: Kinetic Constants for Glucose Analogue Inhibitors

compd no.	substituents at C1 position		concns used (mM)	K_i (mM)	n	α[a]
1	α-OH	β-H	4, 6, 10, 20	1.7 ± 0.1	1.5	0.2
2	α-H	β-OH	10, 20, 40, 60	7.4 ± 0.7	1.5	0.4
3	α-CH_3	β-H	20	53.1 ± 7.6	1.0	nd[b]
4	α-OCH_3	β-H	20, 40, 60	12.0 ± 1.7	1.2	0.5
5	α-H	β-OCH_3	30, 50, 70	24.7 ± 4.0	1.2	0.5
6	α-OCH_2CH_2OH	β-H	3	weak activation		
7	α-H	β-OCH_2CH_2OH	1, 5, 10	25.3 ± 5.6	1.0	0.5
8	α-CH_2N_3	β-H	8	22.4 ± 3.2	1.0	nd
9	α-H	β-CH_2N_3	20, 40	15.2 ± 0.6	1.1	1.0
10	α-OH	β-CH_2N_3	10	7.4 ± 0.6	1.1	0.9
11	α-H	β-$CH_2CH_2N_3$	10	18.7 ± 2.5	1.0	nd
12	α-CH_2OH	β-H	2.5, 5, 8	1.5 ± 0.1	1.3	0.4
13	α-H	β-CH_2OH	20	21.9 ± 3.8	1.2	nd
14	α-OH	β-CH_2OH	10	15.8 ± 2.3	1.0	0.6
15	α-H	β-CH_2CH_2OH	10	15.2 ± 1.7	1.0	nd
16	α-$CH_2OSO_2CH_3$	β-H	5	not inhibitory		
17	α-H	β-$CH_2OSO_2CH_3$	10	4.8 ± 0.4	1.0	nd
18	α-OH	β-$CH_2OSO_2CH_3$	10	3.7 ± 0.2	1.1	0.6
19	α-$CH_2NH_3^+$	β-H	35	34.5 ± 5.8	1.2	nd
20	α-H	β-$CH_2NH_3^+$	8, 4	16.8 ± 5.8	1.0	nd
21	α-H	β-$CH_2CH_2NH_3^+$	5, 3	4.5 ± 0.9	1.0	nd
22	α-H	β-CH_2CN	2, 6	9.0 ± 1.1	1.2	nd
23	α-OH	β-CH_2CN	10	7.6 ± 0.2	1.0	1.1
24[c]		β-*O*(1–6)-D-glucose	20, 30	16.3 ± 2.9		additive

[a] Synergism with caffeine. [b] nd, not determined. [c] Gentiobiose.

Table II: Crystallographic Data Collection and Refinement Statistics

compd	no. of reflcns measd	no. of unique reflcns[a]	$\langle I/\sigma \rangle$	$R_m(I)$[b]	R_{iso}[c]	no. of reflcns used in refinement[d] ($I > 0$)	final R[e]	rms deviation from ideal bond lengths (Å)	rms deviation from ideal bond angles (deg)	rms deviation of glucose core atoms[f] (Å)
1[g]	85 168	34 771	18.5	0.069	0.111	29 240	0.181	0.016	3.4	
6	89 831	33 979	19.3	0.060	0.089					
7	88 621	32 981	14.2	0.078	0.128	31 903	0.231[h]	0.018	3.7	0.36
8	80 398	32 705	17.5	0.067	0.119	30 481	0.193	0.017	3.6	0.20
9	87 799	34 743	15.0	0.072	0.106	33 634	0.204	0.018	3.7	0.30
10	83 482	35 742	15.5	0.073	0.115	34 450	0.203	0.019	3.8	0.23
12	88 619	33 168	16.8	0.065	0.101	32 097	0.194	0.016	3.5	0.29
13	88 235	36 371	15.6	0.069	0.095	35 230	0.195	0.016	3.5	0.17
14	82 660	34 069	16.2	0.072	0.108	32 746	0.203	0.019	3.8	0.17
17	77 095	36 734	16.6	0.072	0.128	35 165	0.207	0.018	3.7	0.32
18	87 606	33 085	14.5	0.073	0.150	34 046	0.210	0.018	3.8	0.16
19	83 529	32 835	15.4	0.073	0.104	31 708	0.192	0.016	3.5	0.19
20	82 530	33 253	14.5	0.076	0.104	32 050	0.198	0.018	3.6	0.29
21	82 835	33 527	15.5	0.073	0.106	32 426	0.193	0.018	3.5	0.25
22	85 768	33 917	13.8	0.079	0.106	32 392	0.195	0.018	3.5	0.41
23	86 368	34 636	14.8	0.076	0.100	33 417	0.199	0.018	3.6	0.37
24	85 901	34 131	10.1	0.099	0.104	33 004	0.196	0.017	3.5	0.22

[a] Data sets were between 75% (32705 reflcns, compound **8**) and 84% (36744 reflcns, compound **17**) complete to 2.3-Å resolution. [b] Merging R factor $R_m = \sum_i \sum_h |I(h) - I_i(h)| / I_i(h)$, where $I(h)$ and $I_i(h)$ are the mean and ith measurement of intensity for reflection h. [c] Mean fractional isomorphous difference in structure factor amplitudes from native T state GP*b*. [d] Reflections between 8- and 2.3-Å resolution. [e] Crystallographic R factor $\sum ||F_o| - |F_c|| / \sum |F_o|$ where $|F_o|$ and $|F_c|$ are the observed and calculated structure factor amplitudes, respectively. [f] Core atoms of glucose analogues defined as C1, C2, O2, C3, O3, C4, O4, C5, O5, C6, and O6. [g] Data from Martin et al. (1990). [h] Water molecules were not included in this refinement.

glucose, respectively. Both the α and β anomers exhibit Hill coefficients (n = 1.5) that indicate a shift in the equilibrium toward the T state. The Hill coefficient in the absence of glucose under the conditions of assay in which GP*b* is activated by AMP is 1.0. The synergism of α-D-glucose is greater than β-D-glucose (α = 0.2 and 0.4, respectively), but there is still significant synergism between the β anomer and caffeine. The importance of the α-1-OH group in binding is shown by the poorer inhibition constants for 1-deoxyglucose (K_i = 10.7 mM; Street et al., 1986) and α-methyl-1-deoxyglucose (K_i = 53 mM, compound **3**, Table I). Both the α and β methyl glucosides are poorer inhibitors than their parent compounds (K_i = 12.0 mM and 24.7 mM, respectively; compounds **4** and **5**, Table I).

None of the glucose analogues studied resulted in improved K_i values compared with glucose but compound **12**, α-hydroxymethyl-1-deoxyglucose, gave comparable value (K_i = 1.5 mM). The kinetic results for this compound are shown in Figure 3. Further discussion of the kinetic results and their interpretation is included with a description of the analogue binding interactions in the crystal structure.

Crystallographic Binding Studies. The crystallographic data collection and the refinement statistics for 14 complexes of GP*b* are summarized in Table II. The data collection and refinements proceeded easily due to well-established protocols on the area detector and the fact that the sugar analogues were designed to stabilize the T state of the enzyme, the form of the enzyme in the tetragonal crystals, and hence there was no

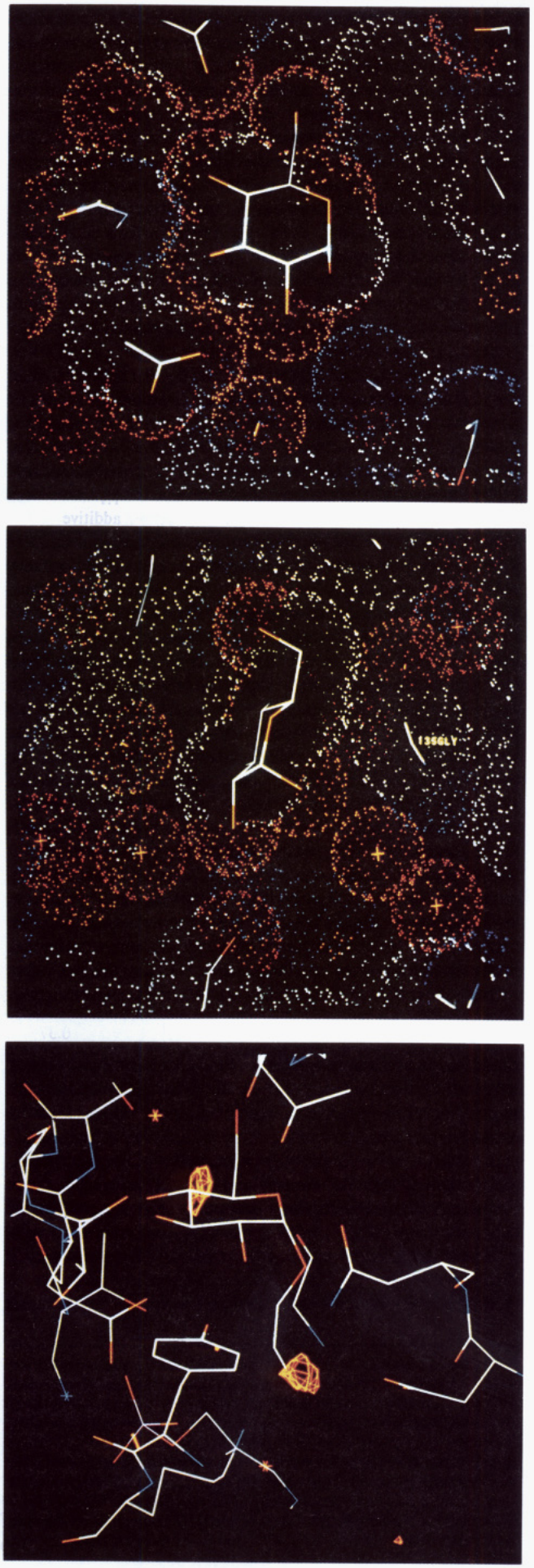

crystal disorder and minor perturbations of the structure. The refined protein structures were essentially identical to the structure of the glucose–GP*b* complex (Martin et al., 1990) and showed the same conformational shifts as the glucose complex from the native unliganded complex (for example, a small shift of His377 away from the glucosyl pyranose moiety). Localized conformational changes at the catalytic site were observed for some of the complexes and these are described later. The errors in the coordinates measured from a Luzzatti plot (Luzzatti, 1952) were about 0.2 Å. The Ramachandran plots and main-chain *B*-factor plots were similar to those that have been described previously for T-state GP*b* (Acharya et al., 1991; Barford et al., 1991). Glucose exhibits an average *B* factor (14 Å^2) that is less than the average *B* factor for the protein CA atoms (20 Å^2).

The positions of the glucose core atoms (C1, C2, O2, C3, O3, C4, O4, C5, O5, C6, and O6) are similar in all compounds studied (Table II). The rms deviation in atomic positions varied from 0.16 to 0.41 Å. The polar contacts to the peripheral hydroxyl groups of the glucopyranose ring are also similar. Hydrogen-bond lengths for glucose and the spread of hydrogen-bonds length for the different analogue complexes are shown in Table III. All exhibit the same pattern: the C2 hydroxyl makes four hydrogen bonds to protein or water atoms but two of these (to Asn284^{ND2} and Tyr573^{OH}) are long and the other two (to Glu672^{OE1} and Wat890) are of moderate length; the C3 hydroxyl has two moderate-length linear hydrogen bonds (to Glu672^{OE1} and Ser674^{N}); there is a long contact from O3 to Ala673^{N} and a bent hydrogen bond to Gly675^{N}; the C4 hydroxyl makes two hydrogen bonds to Gly675^{N} and Wat897 and a contact to Asn484^{OD1} that is too long in all the structures, except the glucose complex itself and those with compounds **19**, **20**, and **21**, to contribute to hydrogen-bond energy; O6 makes a hydrogen bond to His377^{ND1} with rather poor geometry and a longer contact to Asn484^{OD1}; the ring oxygen O5 has polar contacts to Leu136^{N} (3.6 Å) and to His377^{ND1} (3.4 Å) but these contacts are too long and have incorrect geometry for hydrogen bonds. Although the resolution of the data does not allow us to identify hydrogen positions, these were inferred from the known geometry. The likely role of the sugar hydroxyls as hydrogen-bond donors and acceptors and an estimate of the optimum linearity of the hydrogen bonds are given in Table III. Each equatorial hydroxyl acts as both a donor and an acceptor.

The van der Waals contacts between glucose atoms and GP*b* in the glucose complex (Martin et al., 1990) are shown in Table IV. The contacts for the glucose core atoms in the glucose analogue complexes are similar. With the exception of C1, each atom makes several van der Waals contacts. However the 56 van der Waals contacts include only 15 like/like contacts (i.e., polar/polar or nonpolar/nonpolar) and 41 contacts are between unlike groups (i.e., polar/nonpolar). The O3 atom is within van der Waals contact of 11 protein atoms. Nine of these contacts are to nonpolar groups (Figure 1, top). On the other hand, C6 is in contact with eight protein

FIGURE 1: The glucose binding site in GP*b*. (Top) Van der Waals surfaces of the glucose–GP*b* complex viewed face on to the glucopyranose ring. The empty β-pocket is visible lower right. (Middle) Van der Waals surfaces viewed edge on to the glucopyranose ring. The solvent-filled α-pocket is visible lower right. (Bottom) Grid contours for an OH probe with the glucose–GP*b* coordinates for the protein but without waters or glucose, showing potential favorable OH binding sites at −10 kcal/mol. The modeled structure of 1-hydroxyethyl α-D-glucoside (**6**) based on the glucose coordinates is shown superimposed. The view is different from those shown in the panels above.

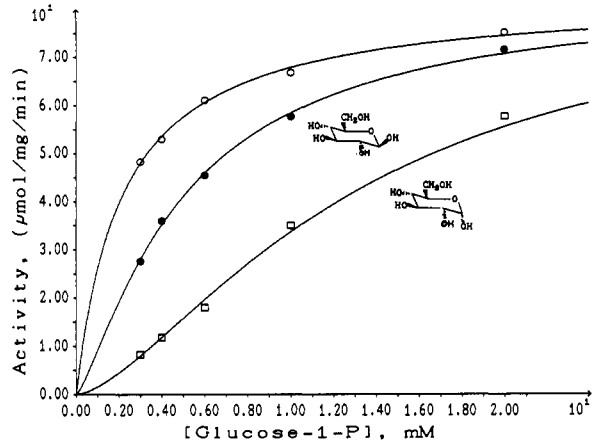

FIGURE 2: The activity of GP*b* at 30 °C and pH 6.8 as a function of substrate concentration in the absence (○) or presence of 10 mM β-D-glucose (●) or 10 mM α-D-glucose (□).

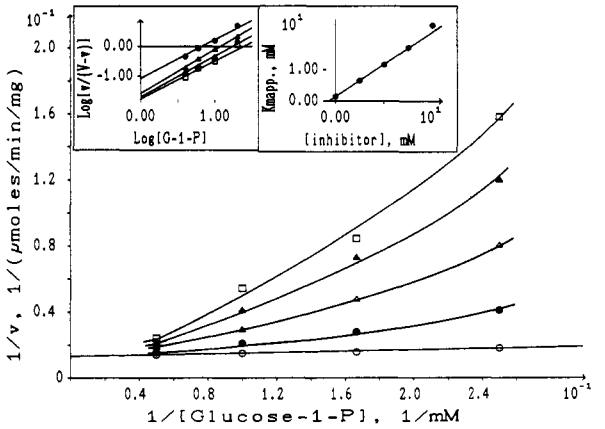

FIGURE 3: Kinetics of α-hydroxymethyl-1-deoxyglucose (**12**) inhibition of GP*b* with respect to Glc-1-P. A double-reciprocal plot of activity and substrate concentration at constant concentrations of glycogen (1%) and AMP (1 mM) and varying concentrations of **12** (0 (○), 5 (●), 10 (△), 15 (▲), and 20 (□) mM) is shown. Inset: Hill plots for Glc-1-P which yielded the apparent K_m for Glc-1-P and Hill coefficient. From the secondary plot of the apparent K_m(app) versus inhibitor concentration, a K_i of 1.5 ± 0.1 mM was measured.

Table III: Polar Contacts between GP*b* and Core Glucose and Glucose Analogue Atoms

glucose atom	glucose donor (D) or acceptor (A)	protein atom	distance (Å)	linearity[a] (deg)	range in glucose analogue complexes[b]
O2	A	ND2 Asn284	3.2	3	3.2–3.3
		OH Tyr573	3.4[c]		3.0–3.5[c]
	D	OE1 Glu672	2.9	6	2.9–3.1
		OH7 Wat890	3.0		2.8–3.2
O3	D	OE1 Glu672	2.9	11	2.7–3.0
		N Ala673	3.4[c]		3.1–3.5[c]
	A	N Ser 674	3.0	5	2.9–3.2
		N Gly675	3.0	48	2.9–3.1
O4	D	OD1 Asn484	3.1	2	3.2–3.6[c]
	A	N Gly675	2.8	6	2.7–2.9
		OH1 Wat897	2.6		2.6–2.7
O6	A	ND1 His377	2.7	32	2.6–2.8
	D	OD1 Asn484	3.0	13	2.8–3.1

[a] Hydrogens were added to glucose and protein atoms with conventional geometry and adjusted, where allowed (e.g., for OH group), to optimize hydrogen-bond geometry. Linearity is defined by the angle H–D–A, where H is the hydrogen on the donor atom D and A is the acceptor atom in a hydrogen bond D—H···A. [b] Glucose analogue complexes included **8**, **9**, **10**, **12**, **13**, **14**, **17**, **18**, **19**, **20**, **21**, **22**, and **23**. [c] Indicates distance too long for a hydrogen bond.

atoms and five of these contacts are to polar groups (Figure 1, middle). Only the group at C5 in the glucopyranose ring

Table IV: Van der Waals Contacts for Glucose Atoms in the Phosphorylase–Glucose Complex

glucose atom	van der Waals contacts[a] (3.0–4.0 Å) with protein atoms	no.
C1	none	0
C2	O His377, OE1 Glu672, OH7 Wat890	3
C3	N Gly675, OE1 Glu672, OH1 Wat897	3
C4	OD1 Asn484, N Gly675, OH1 Wat897	3
C5	CA, C, O Gly135, N Leu136, OH1 Wat897	5
C6	C, O Gly135, CA, N Leu136, CE, ND1 His377, OD1 Asn484, OH1 Wat897	8
O1	CA, C Gly135, N Leu136, ND2 Asn284	4
O2	CG, OD1 Asn284	2
Oe	C, CG, CD Glu672, CA, C, CB Ala673, CA, C Ser674, CA, N Gly675, OH7 Wat890	11
O4	CA, C, CB, OG Ser674, CA, C, O Gly675	7
O5	C Gly135, CA, N Leu136, ND1 His377	4
O6	CD2 Leu139, CG, CE1 His377, CG1 Val455, CG, ND2 Asn484	6
	total	56

[a] Excluding hydrogen bonds.

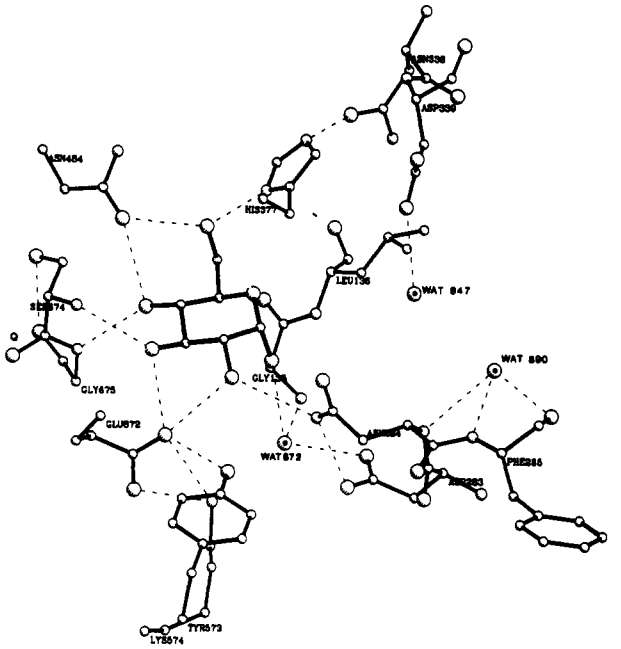

FIGURE 4: Contacts between glucose (**1**) and GP*b*.

is directed toward a complementary group (CA Gly135). This lack of complementarity between polar and nonpolar groups for glucose binding of GP*b* may provide a partial explanation for the apparent weak binding of glucose and is discussed later.

The hydrogen bonds to the substituent atoms at C1 for glucose and the glucose analogue inhibitors are shown in Table V. A summary of the van der Waals interactions, torsion angles, and water molecules displaced is given in Table VI. Glucose makes one hydrogen bond from the α-anomeric hydroxyl to water Wat872^{OH8} (Figure 4). Computation of hydrogen positions indicates this hydrogen bond would be significantly nonlinear if the hydroxyl acted as the donor, and it is assumed that the hydroxyl accepts a hydrogen bond from the water. This water in turn is hydrogen-bonded to Asp283^{OD1}, Gly135^{N}, and Wat879^{OH0}. Compound **6**, hydroxyethyl α-glucoside, was modeled in an attempt to provide a group that would displace this water molecule and form a direct hydrogen bond to the protein. The resulting difference map showed poor binding of **6** to the catalytic site and indicated that the four-atom substitution at the anomeric carbon had displaced the 280s loop toward the R-state conformation. The refinement was halted before inclusion of water molecules.

Table V: Polar Contacts between GP*b* and Substituent Atoms at C1 in Glucose and Glucose Analogue Complexes

compd	atom numbering	ligand atom	protein atom	distance (Å)
1 α-D-glucose	α-O1	O1	OH8 Wat872	3.0
7 1-hydroxyethyl β-D-glucoside	β-O7-C8-C9-O9	O9	OD1 Asp339	2.9
8 α-azidomethyl-1-deoxyglucose	α-C7-N1-N2-N3	N1	N Leu136	3.1
			OH8 Wat 872	3.1
9 β-azidomethyl-1-deoxyglucose	β-C7-N1-N2-N3	N3	OD1 Asp339	2.7
			OH4 Wat847	2.6
10 β-azidomethyl-α-D-glucose	α-O1	O1	OH8 Wat872	3.3
	β-C7-N1-N2-N3	N3	OD1 Asp339	2.9
			OH4 Wat847	2.6
12 α-hydroxymethyl-1-deoxyglucose	α-C7-O7	O7	N Leu136	2.8
			OH8 Wat872	3.1
13 β-hydroxymethyl-1-deoxyglucose	β-C7-O7	none		
14 β-hydroxymethyl-α-D-glucose	α-O1	O1	OH8 Wat872	3.2
	β-C7-O7			
17 β-mesylate-1-deoxyglucose	O81	O81	N Asn284	3.1
	|	O82	OD1 Asp339	2.9
	β–C7–O7–S8–C9			
	|			
	O82			
18 β-mesylate-α-D-glucose	α-O1	O1	OH8 Wat872	3.4[a]
	O81	O81	N Asn284	3.2
	|	O82	OD1 Asp339	2.9
	β–C7–O7–S8–C9			
	|			
	O82			
20 β-aminomethyl-1-deoxyglucose	β-C7-N1	N1	OD1 Asn284	3.2
21 β-aminoethyl-1-deoxyglucose	β-C7-C8-N1	N1	OD1 Asp339	3.2
22 β-cyanomethyl-1-deoxyglucose	β-C7-C8-N8	N8	OH4 Wat847	3.1
23 β-cyanomethyl-α-D-glucose	β-C7-C8-N8	N8	OH4 Wat847	3.2
24 gentiobiose	β(1–6)glucose	O2′	NE2 His341	3.0
		O3′	OH2 Wat890	2.7

[a] Contact long for a hydrogen bond.

Table VI: Summary of Polar Contacts, van der Waals Interactions, and Torsion Angles for Glucose and Glucose Analogue Complexes for Substituent Atoms at C1

compd	K_i[a] (mM)	no. of hydrogen bonds	no. of van der Waals contacts	torsion angles[b] χ^1	χ^2	χ^3	waters displaced
1 α-D-glucose	1.7	1	4				
7 1-hydroxyethyl β-D-glucoside	25.3	1	16	−77	−158	−139	847^{OH4}
8 α-azidomethyl-1-deoxyglucose	22.4	3	22	75	43[c]	−58	
9 β-azidomethyl-1-deoxyglucose	15.2	2	12	−66	177	−179	
10 β-azidomethyl-α-D-glucose	7.4	3	15	−63	180	−179	
12 α-hydroxymethyl-1-deoxyglucose	1.5	2	12	55			
13 β-hydroxymethyl-1-deoxyglucose	21.9	0	7	−65			
14 β-hydroxymethyl-α-D-glucose	5.8	1	11	−63			
17 β-mesylate-1-deoxyglucose	4.8	2	16	−60	−151	155	847^{OH4}
18 β-mesylate-α-D-glucose	3.7	2	17	−55	−149	154	847^{OH4}
20 β-aminomethyl-1-deoxyglucose	16.8	1	8	−90			847^{OH4} 890^{OH2}
21 β-aminoethyl-1-deoxyglucose	4.5	1	10	−74	158		847^{OH4}
22 β-cyanomethyl-1-deoxyglucose	9.0	0	11	−79	−59		890^{OH2}
23 β-cyanomethyl-α-D-glucose	7.0	2	12	−73	56		890^{OH2}
24 gentiobiose	16.3	2	41	−109	171	48	

[a] K_i from Table I. [b] Torsion angles are as follows. **7**: χ^1 = O5–C1–O1–O7, χ^2 = C1–O1–C7–C8, χ^3 = O1–C7–C8–O8. **8**, **9**, **10**: χ^1 = O5–C1–C7–N1, χ^2 = C1–C7–N1–N2, χ^3 = C7–N1–N2–N3. **12**, **13**, **14**: χ^1 = O5–C1–C7–O7. **17**, **18**: χ^1 = O5–C1–C7–O7, χ^2 = C1–C7–O7–S8, χ^3 = C7–O7–S8–C9. **20**, **21**: χ^1 = O5–C1–C7–N1. **22**, **23**: χ^1 = O5–C1–C7–C8, χ^2 = C1–C7–C8–N8. **24**: χ^1 = O5–C1–O1–C6′, χ^2 = C1–O1–C6′–C5′, χ^3 = O1–C6′–C5′–O5′. [c] Strained conformation.

The kinetic results showed that compound **6** augmented the activation of GP*b* by AMP and is not an inhibitor. The modeling studies had been performed with a rigid enzyme and did not take into account the capability of GP*b* for conformational response.

The corresponding β compound **7**, hydroxyethyl β-D-glucoside, bound so that the four substituent atoms partially filled the β pocket and there is a hydrogen bond from O9 to $Asp339^{OD1}$ at the end of the pocket (Figure 5). The structure showed some small shifts in atoms of residues Leu136, Arg569, and Lys574. Despite the appearance of an identical number of hydrogen bonds to the protein compared with α-D-glucose and some 16 van der Waals contacts for the β-substituent atoms, compound **7** exhibited a poorer inhibition constant (K_i = 25.3 mM) compared to glucose (K_i = 1.7 mM). There is an unfavorable contact between $Asn284^{OD1}$ and C8 (3.2 Å) and a slightly unfavorable torsion angle about the C7–C8 bond (Table VI). However, the major contribution to the difference in the binding affinity between **7** and glucose may arise from a loss in conformational entropy. Simple energy calculations using the program AVERAGE (Andrews et al., 1984) indicated that the reduction in binding energy of 2 kcal/mol for compound **7** compared with glucose might be due to the restriction of freedom for rotation about the three bonds of **7** on binding to the enzyme. It was argued that β substituents with more rigid groups might lead to an increase in binding energy.

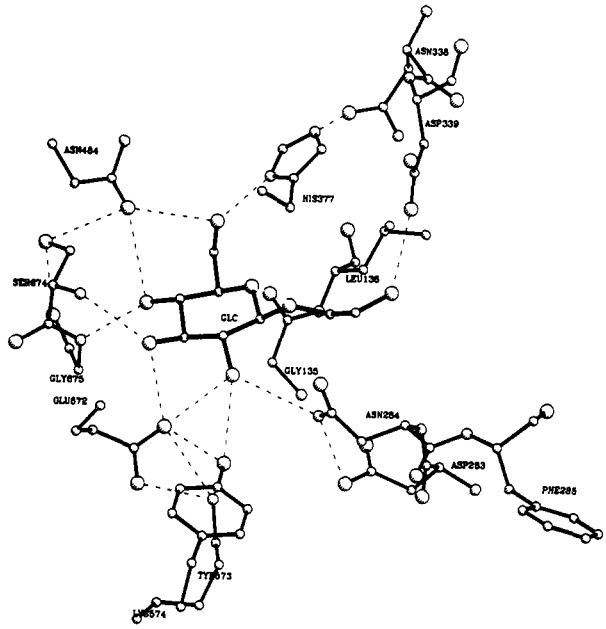

FIGURE 5: Contacts between hydroxyethyl β-D-glucoside (**7**) and GP*b*. Water molecules were not included in this refinement.

Accordingly, the azide series of compounds were prepared. The difference map for compound **8**, α-azidomethyl-1-deoxyglucose, showed the compound bound well, and refinement revealed possible hydrogen bonds between N1 and Leu136^{N} and Wat872^{OH8} and between N3 and Wat847^{OH4}. The azide is sandwiched between the side chains of Leu136 and Asn284, with little change in these residues but small shifts in waters 847^{OH4} and 872^{OH8} and Lys574 side chain. Again, despite these apparently favorable polar contacts and some 22 van der Waals interactions for the α-substituent atoms, compound **8** is a poor inhibitor (K_i = 22 mM). Conformational energy calculations on the refined structure show that **8** has adopted a high-energy conformation compared to the ground-state conformation. The torsion angle C1–C7–N1–N2 = 43° and results in an unfavorable contact between the N2 atom and the H1 atom in the sugar ring. By adopting the unfavorable conformation, the clash between the methyl azido group and Asn284 is avoided and the azide group is placed within the β pocket (Figure 6a).

Compound **9**, β-azidomethyl-1-deoxyglucose, bound as predicted with the β-substituent atoms directed into the β pocket. The C7, N1, and N2 atoms make van der Waals interactions with residues Asn284 and His377, with Leu136, and with Leu136, Asp339, and His377, respectively, with small shifts away from the ligand observed for Asn284 and Leu136 (Figure 6b). The terminal N3 atom is within hydrogen-bonding distance of Asp339^{OD1}, an interaction which would be possible if Asp339 was protonated and the resonance structure of the azide group were such as to place a negative charge on N3 [i.e., C—N=N^{+}=N^{-}···H—O(Asp339)]. The environment of Asp339 is buried with each of the carboxyl oxygens hydrogen-bonded to polar but uncharged groups (His340^{N} and Wat847^{OH4}) and also in van der Waals contact with nonpolar groups from Thr340 and Leu136. In the complex with compound **9**, the water 847^{OH4} is displaced further into the β pocket and remains hydrogen-bonded to Asp339. The refined structure of the GP*b*–**9** complex showed the compound bound in a conformation close to the minimum energy calculation, in contrast to compound **8**. The torsion angle C1–C7–N1–N2 is 177° for **9** (the β anomer) and 43° for **8** (the α anomer). As predicted, the four-atom β-substituted rigid azidomethyl compound **9** showed a smaller inhibition constant (K_i = 15.2 mM) than the more flexible four-atom hydroxyethyl glucoside compound **7** (K_i = 25.3 mM). However, **9** is still a poorer inhibitor than glucose. This may be a consequence of the need for small conformational changes in some side chains in order to accommodate the β-azidomethyl group. Compound **10**, β-azidomethyl-α-D-glucose, was synthesized and tested to explore whether the presence of the α-OH could provide additional binding energy similar to that observed for α-D-glucose. The refined structure of the GP*b*–**10** complex showed identical contacts for the β-azidomethyl group as observed in compound **9** and closely similar conformational shifts. The α-1-OH was hydrogen-bonded to Wat872^{OH8} but the hydrogen-bond length in **10** was slightly longer (3.3 Å) compared to that observed in glucose (3.0 Å). The inhibition

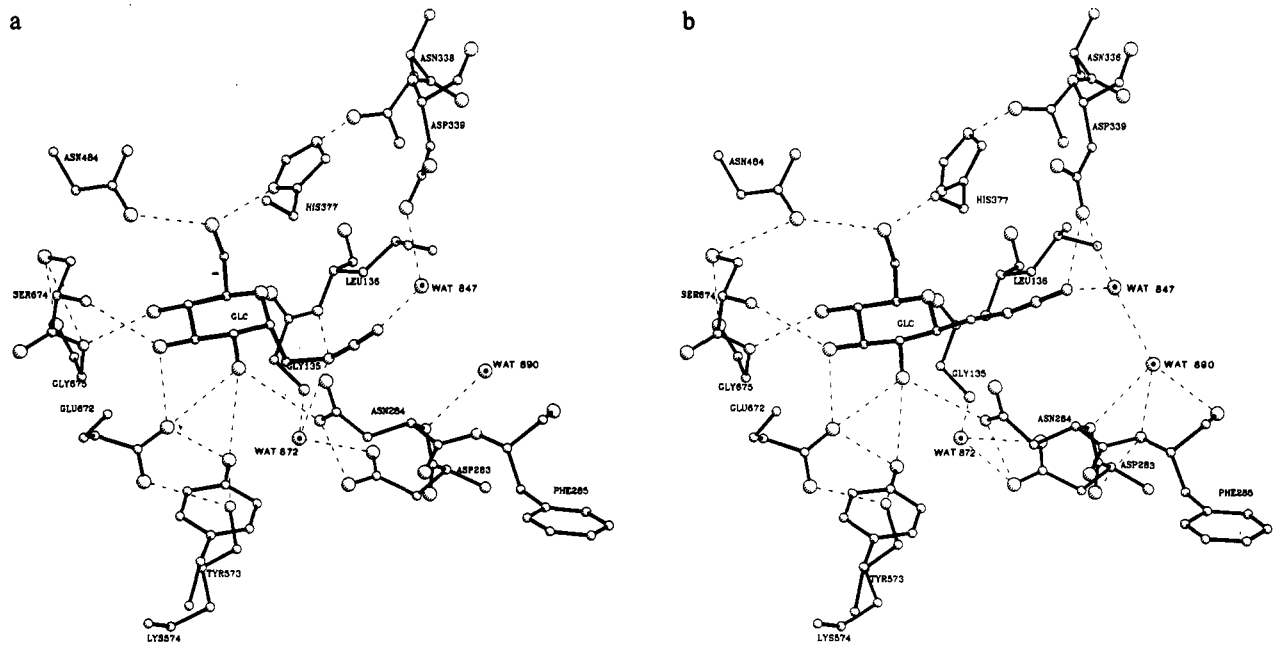

FIGURE 6: (a) Contacts between α-azidomethyl-1-deoxyglucose (**8**) and GP*b*. (b) Contacts between β-azidomethyl-1-deoxyglucose (**9**) and GP*b*.

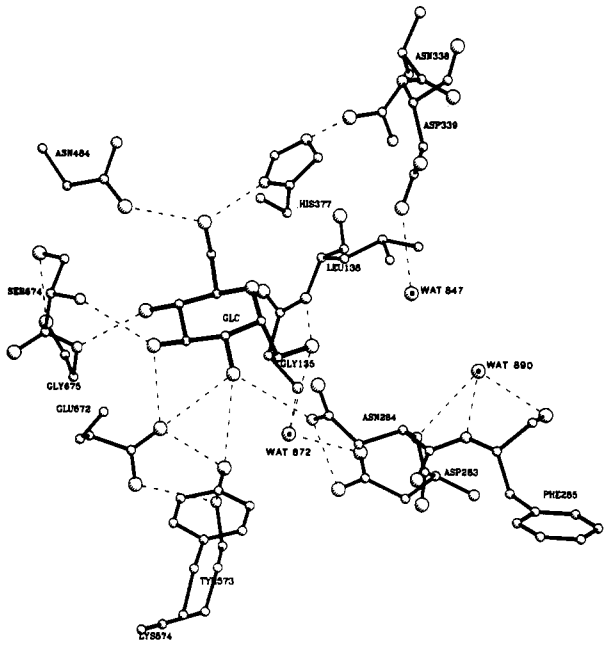

FIGURE 7: Contacts between α-hydroxymethyl-1-deoxyglucose (**12**) and GP*b*.

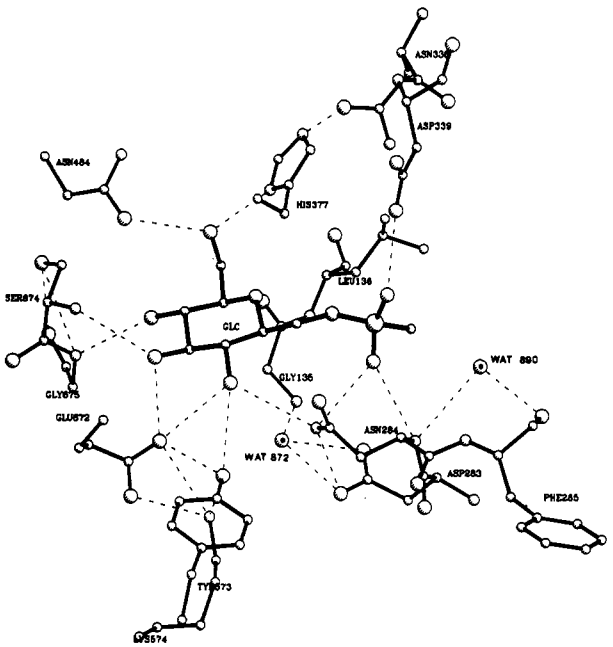

FIGURE 8: Contacts between β-mesylate-1-deoxyglucose (**17**) and GP*b*.

constant for **10** (K_i = 7.4 mM) compared with **9** (K_i = 15.2 mM) indicates that this additional hydrogen bond contributes to the binding energy. However, the β-substituted glucose compound **10** is a poorer inhibitor than glucose. Modeling studies on compound **11**, the β-azidoethyl compound, showed that the β pocket was large enough to accommodate these atoms but that no additional favorable contacts would be made. The inhibition studies showed a poorer K_i than the corresponding methyl compound and crystallographic studies with **11** were not performed.

The results for compounds **6** and **7** stimulated interest in determining the relative binding energies for α and β anomers of shorter hydroxylated substituents at C1. Compounds **12**, **13**, and **14**, in which the hydroxy group is linked by a methylene group to the sugar, were predicted to bind to the protein in low-energy conformations, with the expectation that compound **12** with the α-hydroxymethyl group could make a direct hydrogen bond to the protein. Compound **12** is a good inhibitor (K_i = 1.5 mM; Table I). In the refined structure of the complex the hydroxymethyl group is hydrogen-bonded to Leu136^{N} and to Wat872^{OH8} (Figure 7). The torsion angle O5–C1–C7–O7 = 55° indicates favorable geometry about the C1–O1 bond. The corresponding β compound **13** is a poor inhibitor (K_i = 21.9 mM). The structure indicates a favorable geometry for the torsion angles but the C7 atom makes van der Waals interactions to mostly polar groups (side chains of Asn284 and His377) while the O7 is in van der Waals contact with mostly nonpolar groups (side chain of Leu136) and makes no hydrogen bonds. Compound **14** (β-hydroxymethyl-α-D-glucose) showed an increased affinity compared with **13** (K_i = 15.8 mM compared with 21.9 mM). The hydrogen bond from the O1 atom to Wat872^{OH8} is long (3.2 Å) and is similar to the value observed in the β-azidomethyl (**10**) complex. The β-substituted glucose compound **14** is a poorer inhibitor than glucose.

The mesylate series (compounds **16–18**) are intermediates on the synthetic pathway to several of the other compounds. The α-mesylate **16** ($CH_2OSO_2CH_3$) was not an effective inhibitor and crystallographic binding studies showed no binding, presumably because the substituent atoms clashed with the side chain of Asn284. The β-mesylate, **17**, has a K_i = 4.8 mM.

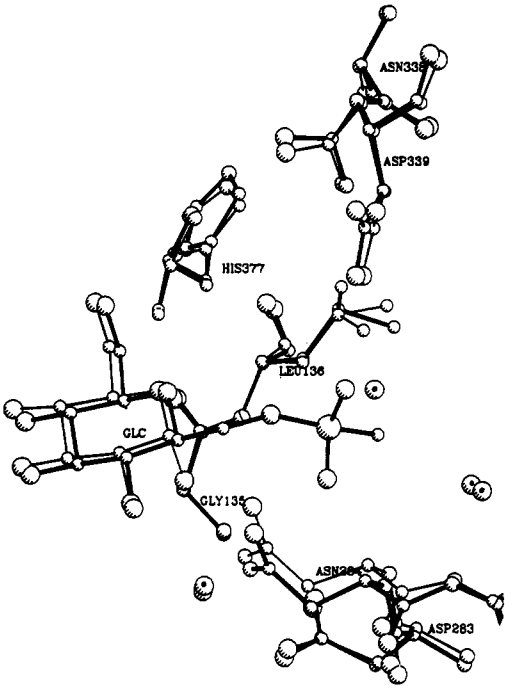

FIGURE 9: Contacts between β-mesylate-1-deoxyglucose (**17**) and GP*b*. The structure of the glucose complex is shown with thin lines.

Crystallographic binding studies showed the mesylate group was accommodated in the β pocket (Figure 8) with satisfactory van der Waals interactions and two additional hydrogen bonds, from O81 to Asn284^{N} and from O82 to Asp339^{Od1}; the latter hydrogen bond requires Asp339 to be protonated as in the β-azidomethyl complexes **9** and **10**. There are good van der Waals interactions between C9 and the side chain of Leu136. Wat847^{OH4} is displaced from the β pocket. The β-mesylate-α-D-glucose, **18**, bound in a manner identical with compound **17** and there was a favorable change in the inhibition constant to K_i = 3.7 mM compared with K_i = 4.8 mM with compound **17**. The additional hydrogen bond in **18** from the α-anomeric hydroxyl to Wat872^{OH8} is long (3.4 Å). The complexes of GP*b* with **17** and **18** show similar changes in conformation from the glucose–GP*b* complex. There are shifts in Asp339 to optimize the contact to the sulfur oxygen and shifts in the side

chains of Leu136 and Thr 378 to improve the contacts to the terminal methyl group. Asn284 shifts away from the substituent atoms (Figure 9).

The mesylate results suggest that it is possible to fill the β pocket with groups that provide additional binding energy and hence exhibit lower K_i values than that observed for β-D-glucose. The presence of the acidic group Asp339 in the β pocket led to the design of the amino series. Compound **19**, α-aminomethyl-1-deoxyglucose, is a poor inhibitor (K_i = 34.5 mM). Crystallographic binding studies showed that the compound bound weakly and there was an unfavorable contact between the amino group and Asn284^{ND2}. In view of the weak binding, contacts for this analogue are not detailed in the tables. Compound **20**, β-aminomethyl-1-deoxyglucose, bound with the side chain accommodated in the β pocket with a potential hydrogen bond to Asn284. The distance from the amino group to Asp339 was too long for an ionic contact and the compound exhibited a poor inhibition constant (K_i = 16.8 mM). Compound **21**, β-aminoethyl-1-deoxyglucose, with the side chain of C–C bond length longer, bound so that the amino group was in satisfactory contact with the OD1 atom of Asp 339 (Table V). This compound is a reasonable inhibitor (K_i = 4.5 mM) and better than β-D-glucose (K_i = 7.4 mM).

The cyanomethyl compounds **22** and **23** were explored to determine the contribution of a three-atom substituent which had rigid geometry. Compound **22**, β-methylcyano-1-deoxyglucose, exhibited an inhibition constant (K_i = 9.0 mM) that was less than that for the β-azidomethyl **9** (K_i = 15.2 mM) but greater than that for the β-aminoethyl **20** (K_i = 4.5 mM), indicating the importance of the interaction of the amino group in the latter complex. Compound **22** bound with satisfactory conformational geometry and van der Waals interactions. Compound **23**, β-cyanomethyl-α-D-glucose, had an improved K_i (K_i = 7.6 mM) compared with **22** (K_i = 9.0 mM). In this complex the hydrogen bond from the α-anomeric hydroxyl to Wat872^{OH8} was 2.7 Å, shorter than that observed in the other β-substituted α-D-glucose compounds. In both the complexes there is a hydrogen bond between the lone pair electrons on the cyano group nitrogen and Wat847^{OH4}. Hydrogen bonds between cyano groups and water have been observed in small-molecule crystal structures (Kurihara et al., 1983).

In a survey of disaccharides, gentiobiose **24** was identified as a potential inhibitor. Modeling studies indicated that the β(1–6) linkage would allow the reducing sugar to bind in the β pocket. This was confirmed by X-ray crystallographic studies (Figure 10). The second sugar was well located and made no short van der Waals interactions to the protein. However, the proximity of Asp339 to the plane of the glucopyranose ring provided an apparent unfavorable polar/nonpolar contact. There were two additional hydrogen bonds (from O2′ to His341^{NE2} and from O3′ through Wat890^{OH2} to Asn284^{N} and Gln285^{N}). The torsion angle O5–C1–O1–C6′ = −109° is closer to the theoretical minimum energy value (−140°) than that observed in the single crystal structure (−58°) (Rohrer et al., 1980). The torsion angle C1–O1–C6′–C5′ = 171° is close to the stable trans conformation. The angle O1–C6′–C5′–O5′ = 48° differs significantly from the single crystal and theoretical values (−62° and −60°, respectively), which would result in steric clash with Asn 284. The conformation observed is within the allowed region and there are no bad intramolecular contacts. The inhibition constant (K_i = 16.3 mM) indicated that gentiobiose is not a potent inhibitor.

Solvent accessibility calculations showed that all glucose analogues were at least 95% buried in the GP*b* complex. The change in solvent accessible area on binding was between 300 Å^2 for the smallest compound (glucose; 98.4% buried) to 320 Å^2 for **18** and 511 Å^2 for gentiobiose (both 97% buried).

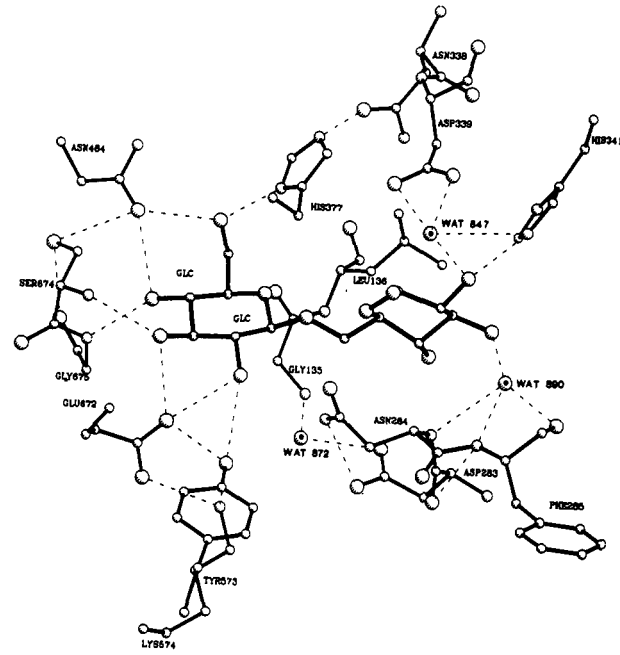

FIGURE 10: Contacts between gentiobiose (**24**) and GP*b*.

Discussion

In the search for better inhibitors of GP*b* than glucose, the important parameters are the K_i and Hill coefficients, which reflect the ability of the inhibitor to compete with substrate for the phosphorylase–AMP–glycogen complex and to favor the T state. The results show that, with the exception of compound **12**, the α-hydroxymethyl analogue, none of the glucose analogues exhibits a lower K_i than α-D-glucose. The analysis provides a comparison between the kinetic inhibition constants and the atomic interactions that occur between the glucose analogue inhibitors and the enzyme and allows some rationalizations. Calorimetric measurements (Steiner et al., 1980) have shown that the binding of glucose to free GP*b* is accompanied by an exothermic change of −6.3 ± 0.5 kcal/mol corresponding to an average dissociation constant of 1.0 mM. This suggests that K_i and K_D are approximately the same for glucose interactions with the enzyme. In the comparative studies, differences in K_i are likely to be directly related to differences in binding energy since the modifications to the basic structure are small. The relative contributions from hydrogen bonds, van der Waals interactions, conformational entropy, conformational energy, water molecules, and charge interactions in determining binding and specificity are summarized.

Glucose Binding. Although not untypical of many carbohydrate-binding proteins, GP exhibits an apparently 10^4-fold lower affinity for glucose than the bacterial periplasmic binding proteins. For effective binding of glucose, the enzyme must provide both sufficient polar contacts to compensate for the transfer of the polar hydroxyl groups from the bulk solvent to the binding site and sufficient complementary nonpolar interactions to the nonpolar CH groups of the sugar ring (Quiocho, 1986; Johnson et al., 1988). Quiocho (1989) has analyzed the features of protein–carbohydrate interactions that contribute to the tight binding of sugars to the bacterial periplasmic binding proteins. For polar interactions he has noted the number of hydrogen bonds, their cooperative nature (simultaneous participation of a sugar hydroxyl as a donor and

as an acceptor), their bidentate nature (two hydroxyls interact with different atoms of the same polar side chain), their favorable hydrogen-bond lengths and angles, the involvement of planar polar side chains that are also involved in networks of hydrogen bonds within the protein, and the large number of charged protein groups involved in hydrogen bonds to the sugar. Comparison of the binding of glucose to the glucose binding protein (GBP; $K_D = 2 \times 10^{-7}$ M) (Vyas et al., 1988) with the binding of glucose to GP*b* shows that many of these features also apply to sugar–phosphorylase binding. The glucose binding site in phosphorylase makes satisfactory polar contacts to almost all of the hydroxyl groups, as noted by Street et al. (1986). There are 13 sugar–protein hydrogen bonds in the glucose–GBP complex and 12 in the glucose–GP*b* complex. With the exceptions of O1, which has only one hydrogen bond, and O5, which is not involved in any hydrogen bonds, the hydroxyl groups of glucose in the glucose–GP*b* complex participate both as donors and as acceptors and all the protein contacts involve planar groups of atoms. The average hydrogen-bond lengths in the GBP-glucose complex and in the GP*b*-glucose complex are similar. The major difference is in the number of hydrogen bonds to charged residues. In the glucose–GBP complex there are seven hydrogen bonds between the hydroxyls and charge residues (involving five charged residues). In the glucose–GP*b* complex there are only three hydroxyl–charged residue hydrogen bonds (involving two charged residues, one of which is a histidine). Fersht et al. (1985) have shown that hydrogen bonds arising from polar–charged interactions are generally stronger by about 2 kcal/mol than those arising from polar–polar interactions.

There is a second important difference between the association of sugars to these two proteins. In both GBP and GP*b* the sugars are buried. In the binding proteins less than 4% of the surface area of the bound sugars is accessible. In phosphorylase, the solvent-accessible area of the bound glucose is 4.8 Å^2, which represents only 1.6% of the accessible area of the free sugar. In GBP there are 47 van der Waals contacts to glucose (excluding the hydrogen bonds), and in GP*b* there are 56 van der Waals interactions to glucose between 3.0 and 4.0 Å. However, in GBP there are striking interactions between the nonpolar components of the glucopyranose ring and two aromatic groups on the protein. The CH groups at C3, C5, and C6 are directed toward Trp183 on one side of the sugar and the CH groups at the C2 and C4 atoms are directed toward Phe16 on the other side. In the GP*b* complex there is very little complementarity between the nonpolar groups of the sugar and nonpolar groups on the enzyme (Figure 1, middle; Table IV) and there are no equivalent aromatic packing interactions. Van der Waals energies are usually treated by a simple distance-dependent energy function that does not take into account the nature of the interactions. A van der Waals contact between two nonpolar groups gives rise to a favorable interaction energy through a fluctuating dipole–induced dipole mechanism. Although extremely weak, these interactions can attain an appreciable energy through resonance if the interacting groups have similar electronic energies. On the other hand, a van der Waals contact between a polar and a nonpolar group (permanent dipole–induced dipole) will be weak because the energy needed to induce the dipole will reduce the energy gained in the interaction. Indeed, the weak binding of fucose to the arabinose binding protein, which is 40-fold weaker than that of arabinose, can be rationalized in terms of an unfavorable nonpolar/water contact (Quiocho et al., 1989) and relaxation of an unfavorable nonpolar/polar contact can lead to an increase affinity (Vermersch et al., 1991). Thus, in the comparison of sugar binding to GBP and GP*b*, the difference in binding energies may arise from the difference in quality of the van der Waals interactions in addition to the strength of the hydrogen bonds. The requirement for complementary van der Waals surfaces is further elaborated in the analysis of the sugar analogue inhibitors of GP*b*.

In GP*b*, one firmly bound water is displaced by the C3 hydroxyl of glucose. The unliganded form of the GBP is not known, so that comparison of water molecules displaced by the sugar cannot be made. In general, it might be expected that the enthalpy lost in breaking the protein–water hydrogen bond would be compensated by the energy gained in making the protein–sugar hydrogen bond but that there might be an overall energy gain from entropic effects on release of the bound water. The bacterial sugar binding proteins exist in an open and closed form and exhibit very low dissociation rates for the ligand. The transformation of T-state GP*b* to R state results in the shift in the 280s loop so that there is a similar open and closed state, although the on and off rates for glucose have not been measured.

α/β Discrimination. These studies have shown that the α anomer of glucose is a more effective inhibitor (K_i = 1.7 mM) than the β anomer (K_i = 7.4 mM), in agreement with the results of others (Cori & Cori, 1940; Street et al., 1986). Analysis of sugar crystal structures has suggested that the anomeric hydroxyl tends to be a strong donor and a weak acceptor in hydrogen bonds when compared with the other hydroxyl groups (Jeffrey, 1990), probably as a result of the anomeric effect (Lemieux, 1963). In the GP*b* complex with α-D-glucose, the α-OH makes a hydrogen bond through a water molecule to Asp283, but the geometry indicates that the α-anomeric hydroxyl acts as an acceptor. Although the binding of β-D-glucose has not been studied crystallographically (because of the problem of mutarotation), the studies suggest that β-D-glucose would bind in a similar way as the other β analogues. The binding mode places the β-OH at a site where there are polar contacts to the side chain of Asn284, but the geometry is wrong for hydrogen bonds, and nonpolar contacts to the side-chain atoms of Leu136 and His377. There are few favorable interactions for the β-OH at this site and there is one less hydrogen bond than in the α-D-glucose complex. Comparison of inhibition constants indicates a difference in binding energy between α- and β-glucose of about 0.9 kcal/mol, an approximate estimate of the strength of the hydrogen bond, if it is assumed that lack of this bond in β-D-glucose is the chief source of difference in binding energy. Further estimates of the strength of this hydrogen bond can be obtained from comparison of the 1-deoxy and α-1-hydroxy pairs of compounds, **9** and **10**, **13** and **14**, **17** and **18**, and **22** and **23**, where the differences in binding energies are 0.4, 0.2, 0.2, and 0.1 kcal/mol, respectively. In these comparisons, however, there will be some loss of energy in the transfer of the α-1-OH group from the solvent to the protein and a possible further loss due to a slight lengthening of the α-1-OH bond in compounds **10**, **14**, and **18** compared with that observed in α-D-glucose, possibly because of constraints imposed by the β substituents. All of the β-substituted α-D-glucose compounds (**10**, **14**, **18**, and **23**) are poorer inhibitors than α-D-glucose, which suggests that occupation of the β pocket results in some unfavorable contributions that are only partially compensated by other contacts.

Environment of the β Pocket. The β pocket is lined by both polar and nonpolar groups and the mixed character of the pocket has presented difficulties in attempts to provide groups

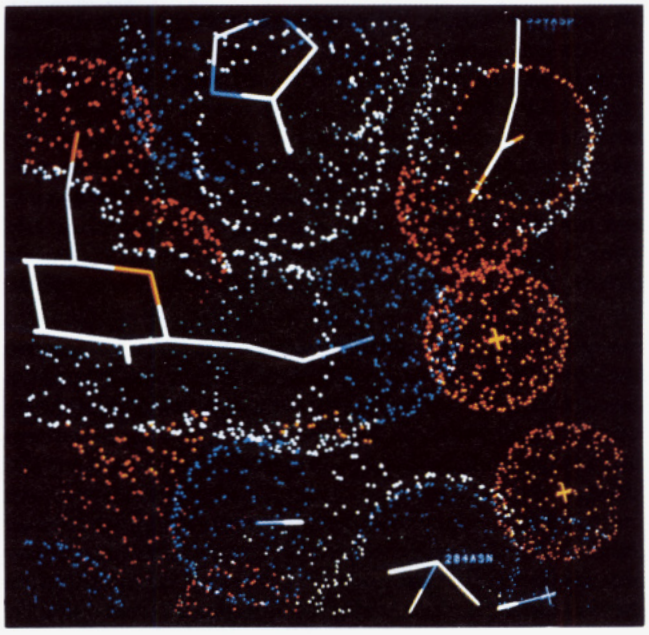

FIGURE 11: Van der Waals surfaces for β-aminoethyl-1-deoxyglucose complex in the vicinity of the C1 substituent atoms which are in contact with Asn284, Asp339, and His377. Leu136 side chain is behind the aminoethyl group in this view. In the native GP*b* structure water $Wat847^{OH4}$ is hydrogen-bonded to Asp339 as shown at the right of the figure. The water is displaced in the aminoethyl-1-deoxyglucose complex.

to facilitate binding (Figure 11). There is no direct correspondence between the number of contacts and the K_i values, but there is some correspondence between the quality of the contacts and the strength of binding (Table VI). For example, the C7 atom of the β-hydroxylmethyl compounds **13** and **14** is in van der Waals contacts to $Asn284^{CG,ND2,OD1}$ and $His377^{C,CB,O}$. Although none of these contacts are less than 3.2 Å, the shifts observed for Asn284 and the proximity of the polar side chain to the C7 group may provide an unfavorable determinant in the binding so that the K_i of **13** is worse than that for β-D-glucose and is not completely compensated by the addition of the α-1-OH group in **14**. The second atom site in the β pocket (i.e., the site that accommodates C8, O7, or N1 for compounds **7**, **9**, **10**, **13**, **14**, **17**, **18**, **20**, **21**, **22**, and **23**) is mostly nonpolar, as determined by the side chain of Leu136, but the side-chain atoms of Asn284 are also in the vicinity. The nonpolar character of this site appears to complement the N1 atom in the β-azidomethyl compounds **9** and **10** and the C8 of the β-aminoethyl (**21**) and cyanomethyl compounds (**22** and **23**) but is less satisfactory for the polar groups of atoms such as O7 in **13** and **14** and the amino group in **20**. The third and fourth atom sites exhibit greater variation as there is more flexibility in the placement of the β-substituent atoms. It is only with the three-atom substituent compound **21** and the four-atom substituent compounds **9**, **10**, **17**, and **18** that a hydrogen-bond interaction to Asp339 can be achieved in the β pocket. In the native GP*b* structure the greater part of the β-channel is empty. This suggests that the environment is suitable neither for polar nor for nonpolar groups; i.e., it cannot be filled either by water molecules or by close packing of complementary groups.

Conformational Entropy and Energy of the Ligand. Compounds whose substituent groups have some inherent flexibility exhibit less favorable binding than compounds containing rigid groups. Compound **7**, with a four-atom flexible group in the β configuration, exhibits a poorer inhibition constant than compound **9**, β-azidomethyl analogue, that contains a similar length four-atom group but with more rigid geometry. Both compounds exhibit an apparent favorable interaction with Asp339 at the end of the β pocket and make a similar number of van der Waals contacts. The most likely source for the difference in binding energies (about 0.3 kcal/mol) is the loss of conformational entropy encountered when the flexible side chain of compound **7** is localized on the enzyme. Compound **22**, the β-cyanomethyl analogue, also contains a more rigid side chain and is a better inhibitor than **7** despite the fact that it has one less atom in the chain for interaction with the enzyme.

The conformational energy of the inhibitor is an important determinant for the overall affinity. The complex with compound **8**, α-azidomethyl analogue, has many van der Waals interactions and two potential hydrogen bonds but exhibits a poor inhibition constant (Table VI). Conformational analysis shows that, of all the compounds studied, the bound conformation of compound **8** is significantly different from the minimum free energy conformation computed from AM1 calculations. The torsion angle about the C7–N1 bond results in unfavorable intramolecular contacts between the N2 and H1 atoms. The unfavorable conformation relieves bad contacts that would be encountered in the minimum free energy conformation between the azido side chain and Asn284. In the complex with compound **8**, a significant portion of the binding energy has been used to compensate the unfavorable conformational energy.

Conformational Changes in the Protein and Displacement of Water Molecules. The most dramatic conformational changes observed were those for the GP*b*–**6** complex, the hydroxyethyl α-glucoside complex. The α-hydroxyethyl group displaced the side chains of Asp283 and Asn284. Shifts in these residues are part of the T to R transition. The conformational changes provide an explanation for the kinetic results that showed compound **6** to be an activator of phosphorylase and not an inhibitor. This result demonstrates some of the difficulties that may be encountered in attempts to predict ligand binding sites on enzymes when the enzyme is modeled as a rigid structure.

In all the β-substituted compounds there were small shifts in the side-chain positions of Leu136, Asn284, Asp339, Thr378, Thr380, and Lys574 of between 0.5 and 1.4 Å. These shifts appeared to be minor adjustments in side-chain positions away from the substituent atoms in order to improve van der Waals interactions. The shifts did not substantially affect the rest of the protein structure. The greatest shifts were found for the two mesylate compounds, **17** and **18**, that have the bulkiest side-chain groups of all the compounds studied. The requirement for the protein to relax in order to accommodate a side-chain group in the β pocket may also be a contributory factor to the generally poor inhibition constants of these compounds. Water 847^{OH4}, which in the native and glucose-complexed GP*b* is hydrogen-bonded to Asp339 at the back of the β pocket, is replaced by polar groups in the complexes with **7** (β-hydroxyethyl), **17** and **18** (mesylates), and **21** (aminoethyl). Thus the enthalpy gained by the ligand–protein hydrogen bond may be almost canceled by the loss in enthalpy of the water–protein hydrogen bond.

Hydrogen Bonds and van der Waals Interactions. Engineering new hydrogen bonds or polar–charged interactions might be expected to lead to the greatest changes in free energy of binding. The results show that this may not happen for a variety of reasons (changes in conformational entropy, changes in conformational energy of the ligand, conformational changes in the protein, displacement of water molecules). Perhaps the

most surprising result is the relatively small increase in binding energy (about 0.8 kcal/mol) between the β-aminomethyl and the β-aminoethyl compounds **20** and **21**, where in the latter compound there is a direct interaction between the amino group and the side chain of Asp339. Structural considerations suggest that Asp339 has a raised pK value and because of its environment may be only partially ionized at the experimental pH of 6.7. The group is removed from the bulk solvent at the end of the β pocket although the OD1 and OD2 atoms exhibit moderate solvent-accessible areas (9.7 and 1.5 Å^2, respectively) because of the space in the β pocket. There are no direct contacts to other charged residues. If Asp339 is partially protonated, then the interaction with the amino group in compound **21** is likely to be less strong than if the Asp339 were ionized. The proximity of the terminal nitrogen of the azidomethyl compounds **9** and **10** to the Asp339 carboxyl group also suggests an interaction that would be stabilized by the protonated form of Asp339 [i.e., C—N=N$^+$=N$^-$...H—O (Asp339)] although other modes of interaction are also possible. In small-molecule crystal structures, the nitrogen–nitrogen bond lengths of the azide group indicate the relative importance of alternative resonance forms may vary (Hossain et al., 1985; Biswas et al., 1987).

α-Hydroxymethyl-1-deoxyglucose (**12**). Compound **12** was modeled and designed in an attempt to displace the water that links α-D-glucose to Asp283 and to replace the interaction by a direct hydrogen bond to the protein. The crystallographic analysis showed that the α-hydroxymethyl compound did not displace the water but did make one direct hydrogen bond to the enzyme (to Leu136^N) in addition to the hydrogen bond to the water. Despite the direct hydrogen bond to the protein, there is little difference in the free energy of binding between α-D-glucose (**1**) and α-hydroxymethyl-1-deoxyglucose (**12**) (K_i = 1.7 mM and 1.5 mM, respectively). Evidently the hydrogen bond through a water molecule contributes as effectively as a hydrogen bond directly to the protein, consistent with the view that firmly bound water molecules in proteins are an integral part of the structure (Baker & Hubbard, 1984; Acharya et al., 1991). The interactions of the α-hydroxymethyl group of **12** are similar to those observed for the GP*b* complex with D-gluconohydroximo-1,5-lactone (K_i = 0.9 mM) (Papageorgiou et al., 1990). In the latter complex the trigonal geometry at C1 places the nitrogen in a polar environment and allows the hydroxyl to hydrogen-bond to Leu136^N.

The detailed structural and kinetic studies illustrate the difficulties that may be encountered in the rational design of drugs. Nevertheless, they also provide guidelines for the design of future ligands that may be better inhibitors. The maximum dose of a therapeutic agent depends on the individual drug but an approximate rule is that the dose should not exceed 20 mg/kg of body weight per day, and to meet these requirements an inhibitor with 10–100 times greater affinity for phosphorylase than the present compounds will be required in addition to the specific requirements concerning uptake, delivery, stability, excretion, metabolism, specificity, and nontoxicity.

References

Acharya, K. R., Stuart, D. I., Varvil, K. M., & Johnson, L. N. (1991) *Glycogen Phosphorylase b*, World Scientific Press, Singapore.

Aebischer, B., Bieri, J. H., Prewo, R., & Vasella, A. (1982) *Helv. Chim. Acta 65*, 2251–2265.

Andrews, P. R., Craik, D. J., & Martin, J. L. (1984) *J. Med. Chem. 27*, 1648–1657.

Angyal, S. J., & Tran, T. Q. (1983) *Aust. J. Chem. 36*, 937–946.

Ariki, M., & Fukui, T. (1977) *J. Biochem. (Tokyo) 81*, 1017–1024.

Austin, P. W., Hardy, F. E., Buchanan, J. G., & Baddiley, J. (1964) *J. Chem. Soc.*, 2128–2137.

Bailey, J. M., & Whelan, W. J. (1972) *Biochem. Biophys. Res. Commun. 46*, 191–197.

Baker, E. N., & Hubbard, R. E. (1984) *Prog. Biophys. Mol. Biol. 44*, 97–179.

Barford, D., & Johnson, L. N. (1989) *Nature 340*, 609–616.

Barford, D., Schwabe, J. W. R., Oikonomakos, N. G., Acharya, K. R., Hajdu, J., Papageorgiou, A. C., Martin, J. L., Knott, J. C. A., Vasella, A., & Johnson, L. N. (1988) *Biochemistry 27*, 6733–6741.

Barford, D., Hu, S.-H., & Johnson, L. N. (1991) *J. Mol. Biol. 128*, 233–260.

Biswas, G., Banerjee, A., & Saenger, W. (1987) *Acta Crystallogr. C43*, 1731–1734.

Bollen, M., Hue, L., & Stalmans, W. (1983) *Biochem. J. 210*, 783–787.

Boobbyer, D. N. A., Goodford, P. J., McWhinnie, P. M., & Wade, R. C. (1989) *J. Med. Chem. 32*, 1083–1094.

Brunger, A. T. (1988) *J. Mol. Biol. 203*, 803–816.

Brunger, A. T. (1989) *Acta Crystallogr. A45*, 42–50.

Brunger, A. T., Karplus, M., & Petsko, G. A. (1989) *Acta Crystallogr. A45*, 50–61.

Cori, G. T., & Cori, C. F. (1940) *J. Biol. Chem. 135*, 733–756.

Cornish-Bowden, A., & Wharton, C. W. (1988) *Enzyme Kinetics*, IRL Press, Oxford, England.

DeFronzo, R. A. (1988) *Diabetes 37*, 667–687.

Dent, P., Lavoine, A., Nakielny, S., Caudwell, F. B., Watt, P., & Cohen, P. (1990) *Nature 348*, 302–308.

Engers, H. D., Shechosky, S., & Madsen, N. B. (1970) *Can. J. Biochem. 48*, 746–754.

Fersht, A. R., Shi, J. P., Knill-Jones, J., Lowe, D. M., Wilkinson, A. J., Blow, D. M., Brick, P., Cortes, P., Waye, M. M. Y., & Winter, G. (1985) *Nature (London) 314*, 235–238.

Fischer, E. H., & Krebs, E. G. (1962) *Methods Enzymol. 5*, 369–372.

Fiske, C. H., & Subbarow, Y. (1925) *J. Biol. Chem. 66*, 375–400.

Goodford, P. J. (1984) *J. Med. Chem. 27*, 557–564.

Goodford, P. J. (1985) *J. Med. Chem. 28*, 849–857.

Hartmann, H., Probst, I., Jungermann, K., & Creutzfeldt, W. (1987) *Diabetes 36*, 551–555.

Helfrich, B., & Johannis, J. (1960) *Annalen 632*, 121–123.

Helmreich, E., & Cori, C. F. (1964) *Proc. Natl. Acad. Sci. U.S.A. 51*, 131–138.

Hers, H. G. (1976) *Annu. Rev. Biochem. 45*, 167–189.

Hossain, M. B., van der Helm, D., Sanduja, R., & Alam, M. (1985) *Acta Crystallogr. C41*, 1199–1202.

Howard, A. J., Gilliland, G. L., Finzel, B. C., Poulos, T. L., Ohlendorf, D. H., & Salemme, F. R. (1987) *J. Appl. Crystallogr. 20*, 383–387.

Jeffrey, G. A. (1990) *Acta Crystallogr. B46*, 89–103.

Johnson, L. N., Cheetham, J., McLaughlin, P. J., Acharya, K. R., Barford, D., & Phillips, D. C. (1988) *Curr. Top. Microbiol. Immunol. 139*, 81–134.

Johnson, L. N., Acharya, K. R., Jordan, M. D., & McLaughlin, P. J. (1990) *J. Mol. Biol. 211*, 645–661.

Jones, T. A. (1978) *J. Appl. Crystallogr. 11*, 268–272.

Jones, T. A. (1985) *Methods Enzymol. 115*, 157–171.
Karjala, S., & Link, K. P. (1940) *J. Am. Chem. Soc. 62*, 917–920.
Kastenschmidt, L. L., Kastenschmidt, J., & Helmreich, E. (1968) *Biochemistry 7*, 3590–3608.
Kasvinsky, P. J., Madsen, N. B., Sygusch, J., & Fletterick, R. J. (1978a) *J. Biol. Chem. 253*, 3343–3351.
Kasvinsky, P. J., Schechosky, S., & Fletterick, R. J. (1978b) *J. Biol. Chem. 253*, 9102–9106.
Kasvinsky, P. J., Fletterick, J., & Madsen, N. B. (1981) *Can. J. Biochem. 59*, 387–395.
Kurihara, T., Uchida, A., Ohashi, Y., Sasada, Y., Ohgo, Y., & Baba, S. (1983) *Acta Crystallogr. B39*, 431–437.
Leatherbarrow, R. J. (1987) *Enzfitter. A Non-Linear regression Data Analysis Program for the IBM-PC*, Elsevier Biosoft, Cambridge, U.K.
Leatherbarrow, R. J. (1990) *Trends Biochem. Sci. 15*, 455–458.
Lemieux, R. U. (1963) in *Molecular Rearrangements* (de-Mayo, Ed.) pp 713–769, Wiley-Interscience, New York, 1963.
Lillioja, S., Mott, D. M., Zawadzki, J. K., Young, A. A., Abbott, W. G., & Bogardus, C. (1986). *J. Clin. Endocrinol. Metab. 62*, 922–927.
Luzzatti, V. (1952) *Acta Crystallogr. 5*, 802–810.
Madsen, N. B., Shechosky, S., & Fletterick, R. J. (1983) *Biochemistry 22*, 4460–4465.
Martin, J. L., Johnson, L. N., & Withers, S. G. (1990) *Biochemistry 29*, 10745–10757.
Melpidou, A. E., & Oikonomakos, N. G. (1983) *FEBS Lett. 154*, 105–110.
Newgard, C. B., Nakano, K., Hwang, P. K., & Fletterick, R. J. (1986) *Proc. Natl. Acad. Sci. U.S.A. 83*, 8132–8136.
Newgard, C. B., Hwang, P. K., & Fletterick, R. J. (1989) *Crit. Rev. Biochem. Mol. Biol. 24*, 69–99.
Noort, D., Veeneman, G. H., Boons, G.-P. P. H., van der Marel, G. A., Mulder, G. J., & van Boom, J. H. (1990) *Synlett*, 205–206.
Oikonomakos, N. G., Melpidou, A. E., & Johnson, L. N. (1985) *Biochim. Biophys. Acta 832*, 248–256.
Papageorgiou, A. C., Oikonomakos, N. G., & Leonidas, D. D. (1989) *Arch. Biochem. Biophys. 272*, 376–385.
Papageorgiou, A. C., Oikonomakos, N. G., Leonidas, D. D., Bernet, B., Beer, D., & Vasella, A. (1991) *Biochem. J. 274*, 329–338.
Pougny, J.-R., Nassr, M. A. M., & Sinay, P. (1981) *J. Chem. Soc., Chem. Commun.*, 375.
Quiocho, F. A. (1986) *Annu. Rev. Biochem. 55*, 287–315.
Quiocho, F. A. (1989) *Pure Appl. Chem. 61*, 1293–1306.
Quiocho, F. A., Wilson, D. K., & Vyas, N. K. (1989) *Nature 340*, 404–407.
Rayment, I. (1983) *Acta Crystallogr. A39*, 102–116.
Roesler, W. J., & Khandelwal, R. L. (1985) *Diabetes 34*, 395–402.
Rohrer, D. C., Sarko, A., Bluhm, T. L., & Lee, Y. N. (1980) *Acta Crystallogr. B36*, 650–654.
Segel, I. H. (1975) *Enzyme Kinetics*, pp 465–504, Wiley Interscience, New York.
Shulman, G. I., Rothman, D. L., Jue, T., Stein, P., DeFronzo, R. A., & Shulman, R. G. (1990) *New Engl. J. Med. 322*, 223–228.
Sprang, S. R., Fletterick, R. J., Stern, M. J., Yang, D., Madsen, N. B., & Sturtevant, J. S. (1982a) *Biochemistry 21*, 2036–2048.
Sprang, S. R., Goldsmith, E. J., Fletterick, R. J., Withers, S. G., & Madsen, N. B. (1982b) *Biochemistry 21*, 5364–5371.
Sprang, S. R., Acharya, K. R., Goldsmith, E. J., Stuart, D. I., Varvill, K. M., Fletterick, R. J., Madsen, N. B., & Johnson, L. N. (1988) *Nature 336*, 215–221.
Stalmans, W., De Wulf, H., Hue, L., & Hers, H. G. (1974) *Eur. J. Biochem. 41*, 127–134.
Steiner, R. F., Greer, L., Bhat, R., & Oton, J. (1980) *Biochim. Biophys. Acta 611*, 269–279.
Street, I. P., Armstrong, C. R., & Withers, S. G. (1986) *Biochemistry 25*, 6021–6027.
Vyas, N. K., Meenakshi, N. V., & Quiocho, F. A. (1988) *Science 242*, 1290–1295.
Witters, L. A., & Avruch, J. (1978) *Biochemistry 17*, 406–410.
Young, A. A., Mott, D. M., Stone, K., & Cooper, G. J. S. (1991) *FEBS Lett. 281*, 149–151.
Zhang, J., Hiken, J., Davis, A. E., & Lawrence, J. C. (1989) *J. Biol. Chem. 264*, 17513–17523.